

AD-A231 367

NAVAL POSTGRADUATE SCHOOL
Monterey, California



THESIS

DTIC
ELECTE
JAN 28 1991
S B D

SATELLITE OBSERVATIONS OF AEROSOL VARI-
ATIONS
IN THE CENTRAL NORTH PACIFIC OCEAN

by

Tod D. Benedict

December 1989

Thesis Advisor

Philip A. Durkee

Approved for public release; distribution is unlimited.

*This document contains color
plates. All DTIC reproductions
will be in black and
white.

Unclassified

security classification of this page

REPORT DOCUMENTATION PAGE

1a Report Security Classification Unclassified			1b Restrictive Markings		
2a Security Classification Authority			3 Distribution Availability of Report		
2b Declassification Downgrading Schedule			Approved for public release; distribution is unlimited.		
4 Performing Organization Report Number(s)			5 Monitoring Organization Report Number(s)		
6a Name of Performing Organization Naval Postgraduate School		6b Office Symbol (if applicable) 35	7a Name of Monitoring Organization Naval Postgraduate School		
6c Address (city, state, and ZIP code) Monterey, CA 93943-5000			7b Address (city, state, and ZIP code) Monterey, CA 93943-5000		
8a Name of Funding Sponsoring Organization		8b Office Symbol (if applicable)	9 Procurement Instrument Identification Number		
8c Address (city, state, and ZIP code)			10 Source of Funding Numbers		
			Program Element No	Project No	Task No
			Work Unit Accession No		
11 Title (include security classification) SATELLITE OBSERVATIONS OF AEROSOL VARIATIONS IN THE CENTRAL NORTH PACIFIC OCEAN					
12 Personal Author(s) Tod D. Benedict					
13a Type of Report Master's Thesis		13b Time Covered From To		14 Date of Report (year, month, day) December 1989	
15 Page Count -- 62					
16 Supplementary Notation The views expressed in this thesis are those of the author and do not reflect the official policy or position of the Department of Defense or the U.S. Government.					
17 Cosati Codes			18 Subject Terms (continue on reverse if necessary and identify by block number)		
Field	Group	Subgroup	Aerosol-Cloud Interaction, AVHRR satellite imagery		
19 Abstract (continue on reverse if necessary and identify by block number)					
<p>A study of aerosol variations in the central North Pacific ocean was conducted utilizing NOAA-9 AVHRR data and concurrent shipboard measurements from the NOAA R/V OCEANOGRAPHER during the RITS-88 cruise. The transect was conducted 7 April to 5 May 1988 along longitude 170° W from latitude 50° N to 12° S. Aerosol physiochemistry measurements were provided every 1° of latitude. Satellite observations of optical depth, Aerosol Particle Size Index, channel 1(0.63 μm) and channel 3(3.7 μm) low cloud reflectances were analysed. These parameters were evaluated during several naturally occurring events, foremost of which were the Gobi desert dust storms and the eruption of Kilauea volcano. By comparing shipboard and satellite data, satellite retrieval techniques were verified, shipboard measurements were expanded to a regional scale, and the relationship between solar reflectance and the microphysical properties of clouds was verified.</p>					
20 Distribution Availability of Abstract			21 Abstract Security Classification		
<input checked="" type="checkbox"/> unclassified unlimited <input type="checkbox"/> same as report <input type="checkbox"/> DTIC users			Unclassified		
22a Name of Responsible Individual Philip A. Durkee			22b Telephone (include Area code) (408) 646-3465		22c Office Symbol 631De

DD FORM 1473,84 MAR

83 APR edition may be used until exhausted
All other editions are obsolete

security classification of this page

Unclassified

Approved for public release; distribution is unlimited

Satellite Observations of Aerosol Variations in the Central North Pacific Ocean

by

Tod D. Benedict
Lieutenant Commander, United States Navy
B.A., The Citadel, 1976

Submitted in partial fulfillment of the
requirements for the degree of

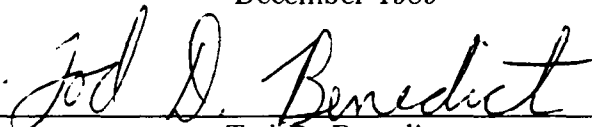
MASTER OF SCIENCE IN METEOROLOGY
AND PHYSICAL OCEANOGRAPHY

from the

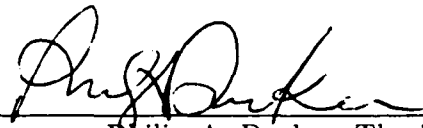
NAVAL POSTGRADUATE SCHOOL

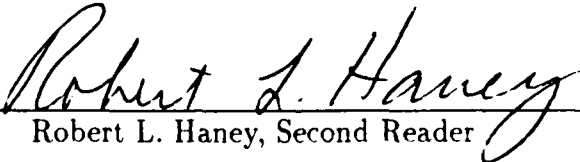
December 1989

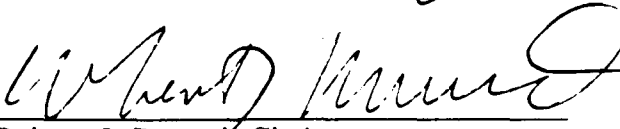
Author:


Tod D. Benedict

Approved by:


Philip A. Durkee, Thesis Advisor


Robert L. Haney, Second Reader


Robert J. Renard, Chairman
Department of Meteorology

ABSTRACT

➤ A study of aerosol variations in the Central Pacific was conducted utilizing NOAA-9 AVHRR data and concurrent shipboard measurements from the NOAA R/V OCEANOGRAPHER during the RITS-88 cruise. The transect was conducted 7 April to 5 May 1988 along longitude 170° W from latitude 50° N to 12° S. Aerosol physiochemistry measurements were provided every 1° of latitude. Satellite observations of optical depth, Aerosol Particle Size Index (S_{12}), channel 1 (0.63 μm), and channel 3 (3.7 μm) low cloud reflectances were analysed. These parameters were evaluated during several naturally occurring events, foremost of which were the Gobi desert dust storms and the eruption of Kilauea volcano. By comparing shipboard and satellite data, satellite retrieval techniques were verified, shipboard measurements were expanded to a regional scale, and the relationship between solar reflectance and the microphysical properties of clouds was verified. ◀

Accession For	
NTIS GRA&I	<input checked="" type="checkbox"/>
DTIC TAB	<input type="checkbox"/>
Unannounced	<input type="checkbox"/>
Justification	
By	
Distribution/	
Availability Codes	
Dist	Avail and/or Special
A-1	

TABLE OF CONTENTS

I.	INTRODUCTION	1
	A. MOTIVATION	2
	B. OBJECTIVES	6
II.	RADIATIVE PROCESSES	8
III.	PROCEDURES	14
	A. DATA ACQUISITION/DESCRIPTION	14
	B. DATA PROCESSING/ANALYSIS	16
IV.	RESULTS	19
	A. SYNOPTIC ANALYSIS	19
	B. AEROSOL SOURCES	24
	C. INTERCOMPARISON OF OPTICAL DEPTH AND CONDEN- SATION NUCLEI	30
	D. INTERCOMPARISON OF S_{12} RATIO AND $NSS-SO_4^{2-}$	35
	E. CHANNEL 1 AND CHANNEL 3 LOW CLOUD REFLECTANCE	40
V.	CONCLUSIONS AND RECOMMENDATIONS	46
	LIST OF REFERENCES	49
	INITIAL DISTRIBUTION LIST	51

LIST OF TABLES

2.1 AVHRR Channel Wavelengths (Kidwell 1986)	9
--	---

LIST OF FIGURES

1.1	Conceptual Diagram of Possible Climate Feedback Loop: the rectangles are measurable quantities and the ovals are processes linking the rectangles	5
2.1	Channel 1 (.63 μm) and channel 3 (3.7 μm) reflectance versus mean droplet radius, from Mineart (1988)	13
3.1	RITS-88 Cruise of R/V OCEANOGRAPHER. Wind vectors are indicated for the Julian Day when data measurements were taken. . . .	15
3.2	Flowchart for Satellite Pixel Processing	17
4.1	NOGAPS 1200 UTC 10 April 1988 Surface Analysis	20
4.2	NOGAPS 1200 UTC 10 April 1988 500 mb Analysis	21
4.3	Number of Clear Observations - Values are within ± 3 days of Ship's Position	23
4.4	"Kosa" Transport Mechanism, 10-14 April 1988, from Murayama (1988) 25	
4.5	"Kosa" Transport Mechanism, 16-20 April 1988, from Murayama (1988) 25	
4.6	Optical Depth Composite. Data taken from NOAA-9 AVHRR during April 1988	27
4.7	S_{12} Composite. Data compiled from NOAA-9 AVHRR during April 1988	29
4.8	Optical Depth - Measured by NOAA-9 AVHRR within ± 3 days of Ship's Position	33
4.9	Condensation Nuclei - Measured by the R/V OCEANOGRAPHER .	34
4.10	S_{12} Ratio - Measured by NOAA-9 AVHRR within ± 3 days of Ship's Position	38

4.11 NSS- SO_4^{2-} Data - Measurements made by R/V OCEANOGRAPHER	
during April 1988.	39
4.12 Channel 1 Low Cloud Reflectance - Measured by NOAA-9 AVHRR .	42
4.13 Composite Optical Depth - Measured by NOAA-9 AVHRR	43
4.14 Composite S_{12} - Measured by NOAA-9 AVHRR	44
4.15 Channel 3 Low Cloud Reflectance - Measured by NOAA-9 AVHRR .	45

ACKNOWLEDGMENTS

I would like to thank Professor Philip Durkee for his assistance, guidance, and support throughout the course of this research. A special thanks to Professor Robert Haney for his careful review of the manuscript. Finally, the staff of the Naval Postgraduate School's Interactive Digital Environmental Analysis (IDEA) Laboratory is commended for their support, especially Mr. Craig Motell. Without his programming skills, this project could not have been completed.

I. INTRODUCTION

The advent of high resolution satellite sensors have allowed for global climate processes to be studied in much greater detail in recent years. Atmospheric elements such as suspended aerosols and various types of clouds interact with the electromagnetic energy within each wavelength band creating unique radiation patterns which the satellite can detect. The scattering and absorption characteristics of these elements are responsible for distinctive radiance signatures. Consequently, information about identifiable atmospheric features may be derived from careful examination of these radiances. With the development of calibrated, multi-channel sensors in conjunction with the great increase in computer power, it is now possible to utilize objective techniques to study the earth's environment with satellites.

Direct observations by ship or aircraft have provided almost the entire body of knowledge concerning aerosol particle distribution over the ocean. Although these data are accurate and useful, it's limited area coverage has been a great problem. Additionally, this data collection process does not allow for long term continuous coverage of a specific area or give the broad coverage necessary for global climate studies.

Satellite remote sensing is currently the only method of continuously monitoring aerosol particles on a global scale. Frost (1988) has developed an algorithm which allows the user to detect aerosol particle characteristics from satellite measurements. Although not able to detect the type of aerosol, measurements can infer the relative size (large or small) of marine aerosol particles in a given volume of air. When correlated with other in-situ data, a good measurement of the spatial and temporal distribution of atmospheric particles occur, and allow for verification

of satellite retrieval techniques. This research will perform such a comparison utilizing aerosol physiochemistry measurements from the Radiatively Important Trace Species (RITS)-88 cruise (Clarke 1989) versus satellite-band NOAA-9 AVHRR measurements for the same time period.

A. MOTIVATION

There are two major motivations for this type of data analysis and the examination of the multi-spectral radiative characteristics of both cloud-free and cloud conditions in the atmosphere. They are separated into a military application and a climate application.

From the military perspective, infrared wavelength image and ranging systems, laser-guided weapons systems, and highly advanced laser communication systems have all demonstrated extreme sensitivity to environmental factors. The molecular and aerosol components of the atmosphere may absorb emitted energy, or scatter a large percentage of it, thereby greatly reducing a military electro-optic systems effectiveness. Milton (1977) worked with infrared wavelength imaging and ranging systems and demonstrated that they are strongly affected by variable distributions of atmospheric aerosols. Shipboard laser-guided weapons with their low level trajectories are especially susceptible to the effects of suspended aerosols. Bloembergen et al., (1987) demonstrated that the optimum wavelength region for any laser system is 0.4-1.0 μm . This wavelength band avoids severe attenuation from atmospheric molecular components at short wavelengths and water vapor absorption at longer wavelengths. However, what must be accounted for in this band is atmospheric aerosols, as they are strong contributors to energy losses. Cordray et al., (1977) conducted operational tests propagating a deuterium fluoride chemical laser

through the lower atmosphere at $3.2\text{ }\mu\text{m}$. The results conclude that aerosol density, size distribution, and chemical and physical composition constitute most of the parameters affecting laser sensitivity. The implications of these results are that real-time microscale measurements of the atmospheric aerosol content is critical for the theater commander to assess and predict the performance of electro-optical systems. Knowledge of the characteristics and locations of aerosol features is vital to determining the sensor settings, weapon paths, and launch/no-launch criteria. Clearly the availability of these data would greatly enhance a mission's success percentage.

From the climatic perspective, the scattering and absorption of solar radiation by aerosol particles and clouds influences the earth's radiation budget and thus can have a significant impact on climate variations. Various hypotheses have been proposed describing both a global warming and cooling trend. The "greenhouse effect", absorption by the atmosphere of infrared energy emitted from the earth, has been the most publicized theory for a global warming trend. Additionally, deforestation and volcanic eruptions have been proposed as planetary sources for warming/cooling. Twomey et al., (1984) suggests that increased atmospheric pollution may lead to a general cooling trend due to increases in small aerosol particles in the atmosphere. Increases in aerosol concentration lead to increases in the number of cloud concentration nuclei (CCN). Assuming a constant liquid water content (LWC), the increase in CCN increases the number of cloud droplets and decreases the droplet radius. This results in increased reflection of incoming short-wave radiation and thus a global cooling trend. At the same time, high cirrus clouds have the ability to increase absorption of outgoing terrestrial long-wave radiation, thereby warming the earth. Thus, an important climatic dilemma exists; clouds both reflect incoming short-wave radiation (cooling effect) and absorb outgoing long-wave radiation (warming effect). Atmospheric temperature fluctuations indicate that many processes are operating

to produce the observed mean annual temperature. Coakley et al., (1983) showed that the effect of aerosols on the earth's radiation budget, through their influence on clouds, may be several times that of the direct interaction of the aerosol with solar radiation. Due to the extreme complexity and spatial variability of clouds, most climate models tend to neglect or over-simplify intricate environmental processes which tend to control climate.

One such important process is described by Charlson et al., (1987) and is represented by Fig. 1.1. He proposes that the majority of CCN formed in remote, marine regions are due to aqueous dimethylsulfide (DMS) emissions through a series of complex biological, chemical, and physical processes. The rectangles in Fig. 1.1 represent measurable quantities, while the ovals represent processes that may or may not be fully understood. DMS is excreted by marine phytoplankton found throughout the planet's aquatic environment. This DMS is then ventilated to the atmosphere via an air-sea transport mechanism where it undergoes an oxidation process. The result of this chemical reaction is the formation of two products: a methane sulfonate (MSA) and a sulfate. The sulfate is thought to be the main product and undergoes a transformation to non sea-salt sulfate ($NSS - SO_4^{2-}$) particles.

The abundance of these aerosols in the marine layer support Charlson's hypothesis that these are the principal CCN particles. Observations by Pruppacher and Klett (1978) demonstrated that observable CCN concentrations vary from 30 to 200 cm^{-3} whereas the sea-salt particle concentrations are usually not greater than 1 cm^{-3} . Therefore, sea-salt particles cannot be the main CCN source. Two possibilities now exist for the $NSS - SO_4^{2-}$. First, they may add mass to the existing CCN which would tend to increase the particle radii. Conversely, these particles

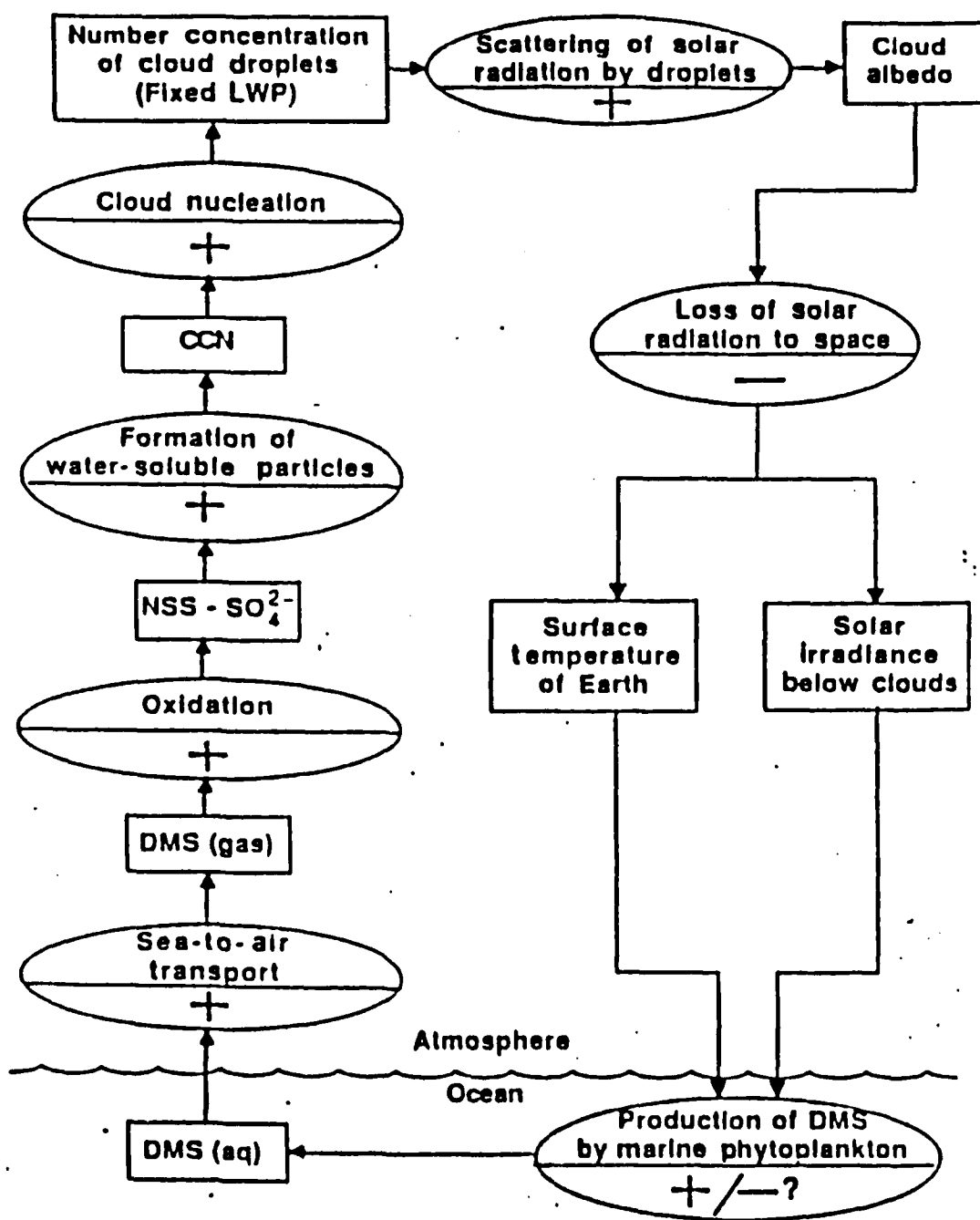


Figure 1.1: Conceptual Diagram of Possible Climate Feedback Loop: the rectangles are measurable quantities and the ovals are processes linking the rectangles.

could create new and hence smaller CCN. This resultant change in size distribution would then affect the reflectance characteristics of the cloud. Twomey (1977) showed that this decrease in droplet radius leads to an increase in the total surface area and thus an increase in the cloud albedo. This implies that oceanic biological variability may play a major role in marine cloud albedo changes and thus in planetary climatic trends.

Identification of variable aerosol contributions to the radiative properties of cloud fields, such as continental pollution sources, volcanic sources, and DMS production is a major motivation for conducting this research.

B. OBJECTIVES

Satellite measurements of aerosol particles can provide a better understanding of the complex interrelationship between the atmosphere and the ocean. The primary objective of this thesis is to provide a verification of satellite retrieval techniques with regards to aerosol particle characteristics. Pfeil (1986) with modifications from Frost (1988) utilized the satellite measured red and near infrared radiance to infer the size relationship of aerosol particles. This is accomplished by forming a ratio of the albedos, as determined from these two wavelengths.

The second objective is to utilize the ship-based observations recorded during the RITS-88 cruise and expand the data to regional scales utilizing the NOAA-9 AVHRR satellite in the visible, near infrared and infrared portions of the electromagnetic spectrum. The two primary areas of interest are at 20° N and 40° N, where large concentrations of aerosol particles exist. The identification of the sources for these aerosols will be shown using satellite retrieval methodology.

Finally, the relationship between aerosol characteristics and cloud reflectance properties will be verified. Mineart (1988) demonstrated the ability to deduce cloud

microphysical parameters (primarily mean cloud droplet size distribution) of marine stratocumulus clouds utilizing AVHRR satellite data. A multispectral image processing technique is used which combines AVHRR channels 1 ($0.63\ \mu\text{m}$), 3 ($3.7\ \mu\text{m}$), and 4 ($10.9\ \mu\text{m}$) to obtain reflectance values. These reflectance values, obtained from the same region as the RITS-88 cruise data, will allow for a determination of the relationship between solar reflectance and the microphysical properties of stratocumulus clouds.

II. RADIATIVE PROCESSES

Radiant energy propagating through the earth's atmosphere is attenuated by interactions with gaseous molecules, suspended aerosols, and the cloud's and earth's surface. This attenuation, which includes absorption and scattering, is highly dependent on such factors as electromagnetic wavelength and the composition of the atmosphere. The AVHRR sensor located on the NOAA-9 satellite measures wavelengths in five channels, each of which is located in an atmospheric absorption "window", where the incoming electromagnetic energy is primarily affected only by scattering. Table 2.1 gives a complete listing of the channels and respective wavelengths. Channel 5 thermal emittance measurements will not be utilized in this thesis.

Backscattered and emitted radiance measured by the AVHRR can provide significant information about atmospheric and surface features. Because each channel detects radiant energy in a separate wavelength band, different characteristics of these features are revealed based on scattering properties of aerosols. Suspended aerosol quantities and size distributions along with several cloud characteristics, primarily cloud thickness and liquid water content (LWC), are revealed by the measurements of channel 1 and channel 2 (Frost 1988). Channel 3 radiance measurements provide different cloud properties, such as the number of droplets and their size distribution, which may be inferred from cloud concentration nuclei (CCN) characteristics. Channel 4 radiance measurements provide an indication of surface and cloud-top temperatures. The analysis of these four channels provide powerful tools for studying aerosol and cloud parameters.

TABLE 2.1: AVHRR Channel Wavelengths (Kidwell 1986)

CHANNEL	RADIANCE	WAVELENGTH BAND
1	Visible	0.58 - 0.68 μm
2	Red visible/Near infrared	0.70 - 1.10 μm
3	Near infrared	3.50 - 3.90 μm
4	Thermal infrared	10.30 - 11.50 μm
5	Thermal infrared	11.30 - 12.40 μm

Optical depth is the first aerosol parameter to be discussed. Because satellites detect upward scattered radiation from aerosol particles, as upwelled radiance, Durkee et al., (1986) showed that there is a direct correlation between the upwelled radiance measured at the satellite and the aerosol particle optical depth. When the optical depth is linked to the size and distribution of aerosol particles, it is possible to relate the satellite detected radiance to the size distributions of the marine aerosols. Optical depth is defined as

$$\delta = \int_0^H \beta_{ext} dz \quad . \quad (2.1)$$

This is the extinction coefficient of the entire atmosphere integrated from the surface to the satellite. The extinction coefficient is given by

$$\beta_{ext} = \int_0^\infty \pi r^2 Q(m, r) n(r) dr \quad , \quad (2.2)$$

where πr^2 is the cross-sectional area of the particle and $n(r)dr$ is the size distribution of the particle at the cross-sectional area. Q_{ext} is an extinction efficiency factor that varies with the radius (r) and composition through the index of refraction (m).

Equations (2.1) and (2.2) show the relationship between optical depth and the aerosol particle. β_{ext} is a function of aerosol particle size and distribution. Because optical depth is a function of β_{ext} , it follows that changes in aerosol particle size or distribution will be reflected in optical depth and satellite-detected radiance.

When aerosol particles change, there also must be changes in the radiative properties of the atmosphere. Durkee (1986) clearly shows that any change in the optical depth results in a change in the diffuse upward radiance at the top of the atmosphere. Additionally, optical depth is a function of the single scattering albedo, satellite zenith angle, solar radiation, and scattering phase function. Based upon the previous assumptions, satellite zenith angle and phase function are the major variables in determining optical depth. Durkee (1984) showed that satellite zenith angle is the most critical factor affecting the radiance-optical depth relationship for small scale analysis. Frost (1988) proved that a variable phase function, such as the Heney-Greenstein scattering phase function, should be utilized on large scale optical depth analysis where large changes in aerosol particle distributions are expected. Because optical depth is calculated with a phase function that varies with the dominant aerosol particle, a more accurate representation is obtained.

The second aerosol parameter to be discussed is the relationship between radiance and the aerosol size distribution. Durkee (1984) showed that the aerosol particle dependent terms in the radiative transfer equations (RTE) are larger at red wavelengths (channel 1) than at near infrared wavelengths (channel 2). Because diffuse radiance is proportional to aerosol particle dependent terms, spectral variations in radiance result from variations in aerosol particle dependent terms. This ratio, labeled the aerosol particle size index (S_{12}) is quantified, as

$$S_{12} = \frac{(L_A)_{red}}{(L_A)_{nir}} \approx \frac{(\delta A)_{red}}{(\delta A)_{nir}} , \quad (2.3)$$

where δ_A is the optical depth due to aerosol particles. The ratio of channel 1 to channel 2 reflectance enhances the variation between aerosol size distributions in the cloud-free atmosphere. More small particles will display a significantly greater difference between channel 1 and channel 2 than a size distribution weighted toward more large particles. Although satellite derived measurements cannot provide the actual particle size distribution curve, the greater the S_{12} ratio, the greater the influence of small particles relative to large particles in the atmosphere and vice-versa.

The final aerosol parameter to be discussed is the change in the cloud reflectance properties based on CCN/aerosol variations. To evaluate these changes, it is necessary to evaluate both the AVHRR channel 1 and channel 3 reflectance. For channel 1, since there is no absorption at this wavelength, incoming photons are either transmitted through the cloud or scattered by cloud droplets and reflected. If the cloud thickness is increased, there is less likelihood that energy will be transmitted through the cloud, thus increasing backscattered radiation. If the LWC is increased, backscattered energy will also increase due to more interactions between photons and cloud droplets. Therefore, channel 1 reflectance is a function of size distribution, cloud thickness, and LWC. This makes it very difficult to assess variations in reflectance values without making limiting assumptions.

Conversely, for channel 3 reflectance, the dependence on LWC and cloud thickness is not nearly as great as the dependence on droplet radius. The sensitivity of reflectance to droplet radius in channel 3 is greatest, due to the moderate absorption at $3.7 \mu\text{m}$ (Coakley and Davies 1986). Therefore, there is virtually no transmission through the cloud at this wavelength. This means that LWC and cloud thickness variations do not appreciably affect the cloud reflectance. This allows one to

conclude that, at channel 3 wavelengths, the reflectance would increase based on injection of smaller CCN which leads to smaller and more numerous cloud droplets.

Mineart (1988) further illustrated this point by comparing strato-cumulus cloud reflectance to mean droplet radius at both channel 1 and channel 3 wavelengths. Fig. 2.1 shows the results of these measurements. There is no correlation of channel 1 with droplet size because of the competing effects of size distribution with cloud thickness and LWC. For channel 3 reflectance values, as expected, a strong linear correlation occurs. As the mean droplet radius increased, the channel 3 reflectance values decreased, indicating that changes in cloud reflectance based on size distribution are observable in channel 3.

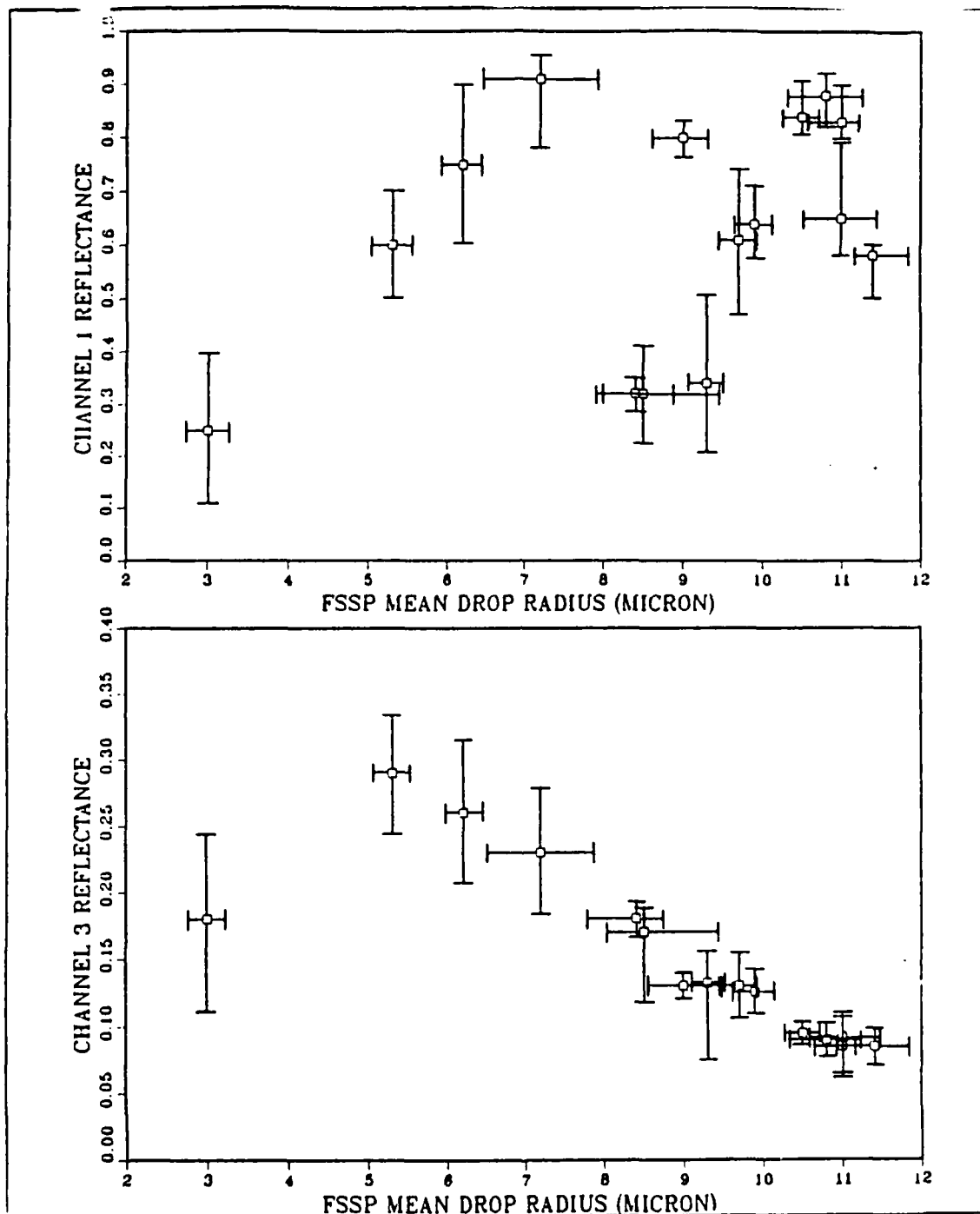


Figure 2.1: Channel 1 ($.63 \mu\text{m}$) and channel 3 ($3.7 \mu\text{m}$) reflectance versus mean droplet radius, from Mineart (1988)

III. PROCEDURES

A. DATA ACQUISITION/DESCRIPTION

The satellite data used in this thesis were obtained from the National Environmental Satellite Data and Information Service (NESDIS) digital archives. The data were collected by NOAA-9, a sun-synchronous near polar orbiting satellite with a nominal altitude of 833 km. Upwelled radiance was measured by the Advanced Very High Resolution Radiometer (AVHRR) sensor on the satellite. Maximum resolution of data at the satellite sub-point is 1.1 km x 1.1 km. Global Area Coverage (GAC) data were examined during the period 7 April - 5 May 1988. The use of GAC data, which minimizes archiving requirements, reduces the resolution to approximately 4.0 km x 4.0 km. The primary area of concern for this thesis is a remote marine region bounded by 50° North and 20° South latitude and 175° and 165° West longitude.

The Shipboard measurements were obtained from the R/V OCEANOGRAPHER, a National Oceanic Atmospheric Administration (NOAA) funded research vessel, during the Radiatively Important Trace Species (RITS)-88 cruise conducted 7 April 1988 to 5 May 1988. Sampling began at 50° N latitude and terminated at 12° S latitude along longitude 170° W. A complete ship's track is displayed in Fig. 3.1 along with wind observations. Data measurements were obtained for every 1° of latitude and consisted of Dimethyl Sulfide (DMS) emissions in the sea and air, $NSS - SO_4^{2-}$ aerosol concentration, aerosol size distribution, and total particle concentration (Bates and Charleson 1989).

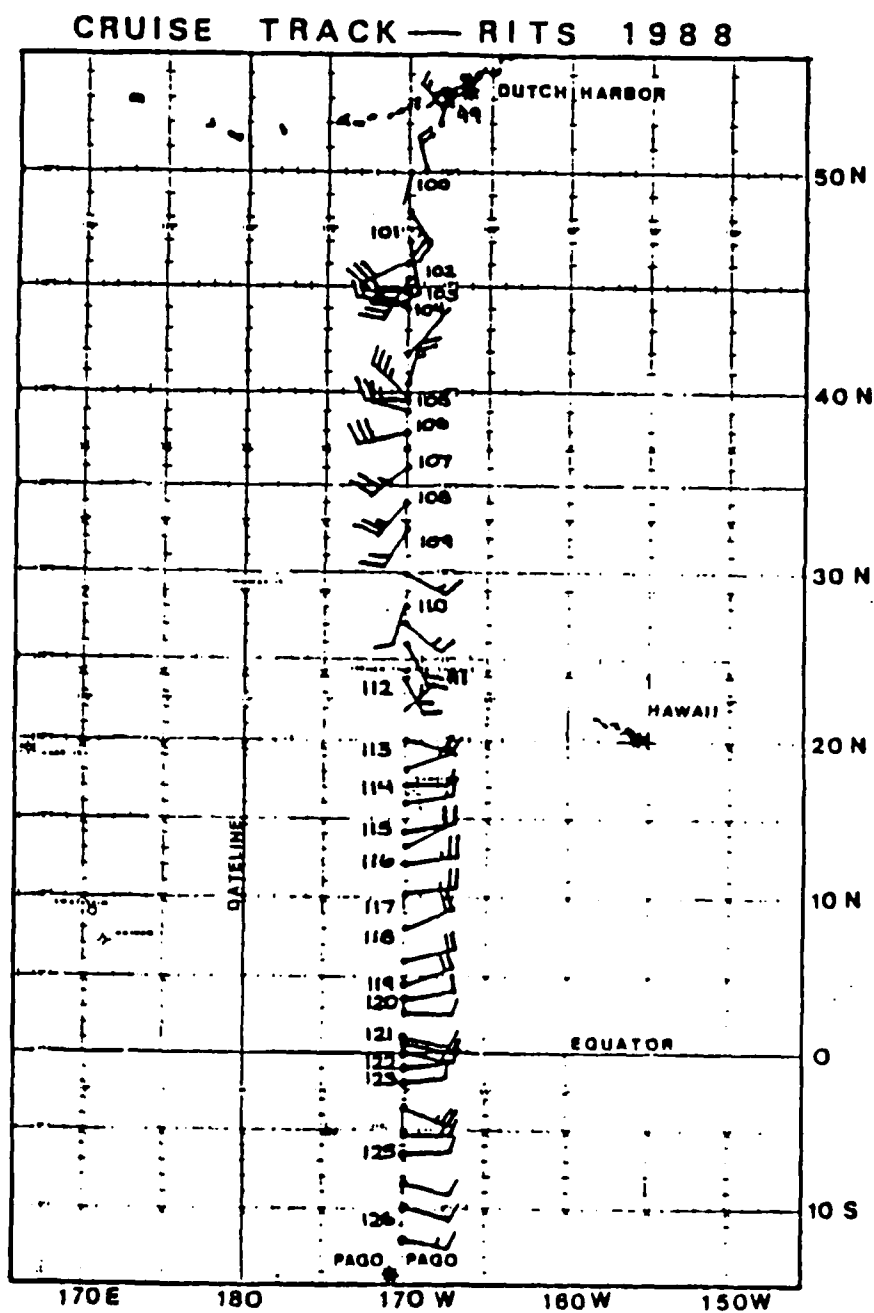


Figure 3.1: RITS-88 Cruise of R/V OCEANOGRAPHER. Wind vectors are indicated for the Julian Day when data measurements were taken.

B. DATA PROCESSING/ANALYSIS

Processing was performed at the Naval Postgraduate School's Interactive Digital Environmental Analysis (IDEA) Laboratory located in Monterey, California. The AVHRR satellite data were processed in order to derive the desired reflective and thermal parameters and to produce the associated images. Each of the six NOAA-9 GAC tapes (72 individual satellite passes) processed required approximately 19 hours of CPU time per tape to obtain the necessary data to cover the entire area of the RITS-88 cruise.

The AVHRR data were analyzed based on a scheme developed by Pfeil (1986) and modified by Frost (1988). Fig. 3.2 is the flowchart by which the data were processed. The applicable data sets produced from this algorithm are as follows:

1. Channel 1/Channel 2 radiance ratio for cloud-free atmosphere.
2. Channel 1 reflectance for low clouds.
3. Channel 3 reflectance for low clouds.
4. Optical depth using a variable Heney-Greenstein phase function for cloud-free atmosphere.
5. Number of partly cloudy pixels.
6. Number of high cloud pixels.

Results for each data set were stored and averaged in $1^\circ \times 1^\circ$ boxes. The number of pixels in each box varied depending upon the series of pixel tests in accordance with Fig. 3.2.

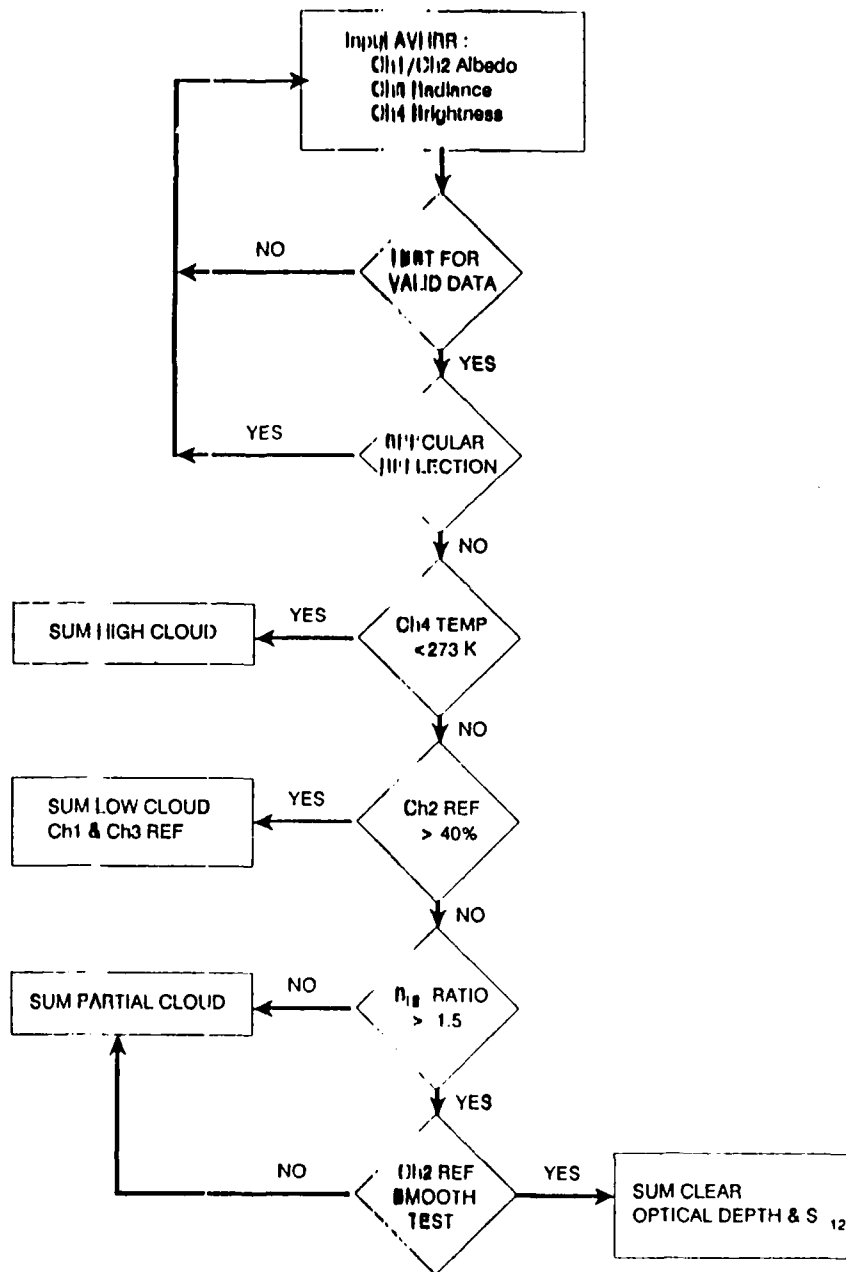


Figure 3.2: Flowchart for Satellite Pixel Processing

The first test in the algorithm averaging process is to verify that the input AVHRR pixel is valid. This is done by determining if the channel 2 or channel 4 radiance values are greater than zero after Rayleigh radiances have been removed. If less than zero, the input pixel is not processed. The next test is to check for contamination due to specular reflection. Because sunglint is a function of satellite viewing geometry, it is removed by calculating an elliptical shaped viewing area. If sunglint contamination is present, the pixel is not processed. The third test in the algorithm is to determine if the pixel is contaminated by high clouds. Should the channel 4 brightness temperature be less than 273 K, then the pixel is considered to be high cloud contaminated and summed in the high cloud data set. The next test performed is a check for low cloud contamination. If the channel 2 cloud albedo is greater than 40%, it is considered a low cloud pixel and summed in the channel 1 and channel 3 reflectance data sets. The fifth test in the series is a preliminary check to identify clear pixels. If the channel 1/channel 2 (S_{12}) albedo ratio is greater than 1.5, then the pixel is tentatively classified as clear, and is subjected to the smooth test for final determination. If not, it is summed in the partly cloudy pixel data set.

The smooth test consists of finding the maximum and minimum channel 2 albedo raw counts for the four pixels surrounding the pixel in question. If the difference between the maximum and minimum pixels is less than or equal to 5, the pixel passes the smooth test, and is summed in the optical depth and (S_{12}) data sets. Otherwise, the pixel is flagged as a partly cloudy pixel, and the process continues until all pixels on the data tape have been accounted for. From these data sets, the final $1^\circ \times 1^\circ$ images are produced for comparison against the surface shipboard data collected by the R/V OCEANOGRAPHER.

IV. RESULTS

This section describes the results obtained from the satellite measurements and the shipboard observations. First, a brief introduction to the synoptic weather situation, major environmental factors, and color-enhanced composite images for optical depth and Aerosol Particle Size Index (APSI) for the entire region will be discussed. Second, comparisons between shipboard data and satellite data will be presented. The satellite data utilized is within a $\pm 5^\circ$ longitude band and ± 3 days of ship's position during data collection. The comparison discussions are:

- Satellite derived optical depth measurements compared to the shipboard measurements of condensation nuclei (CN)
- The Aerosol Particle Size Index (channel 1/channel 2 ratio) compared to the shipboard measurements of atmospheric NSS-SO_4^{2-} concentrations
- Channel 1 and Channel 3 low cloud reflectance values for the entire observation period

A. SYNOPTIC ANALYSIS

Understanding the synoptic weather pattern is critical to determining the source of aerosol particles in this region. Identifying this source helps to explain the results obtained from both the satellite and shipboard data. Fig. 4.1 and 4.2 display a representative surface and 500 mb synoptic flow pattern for the April 1988 period.

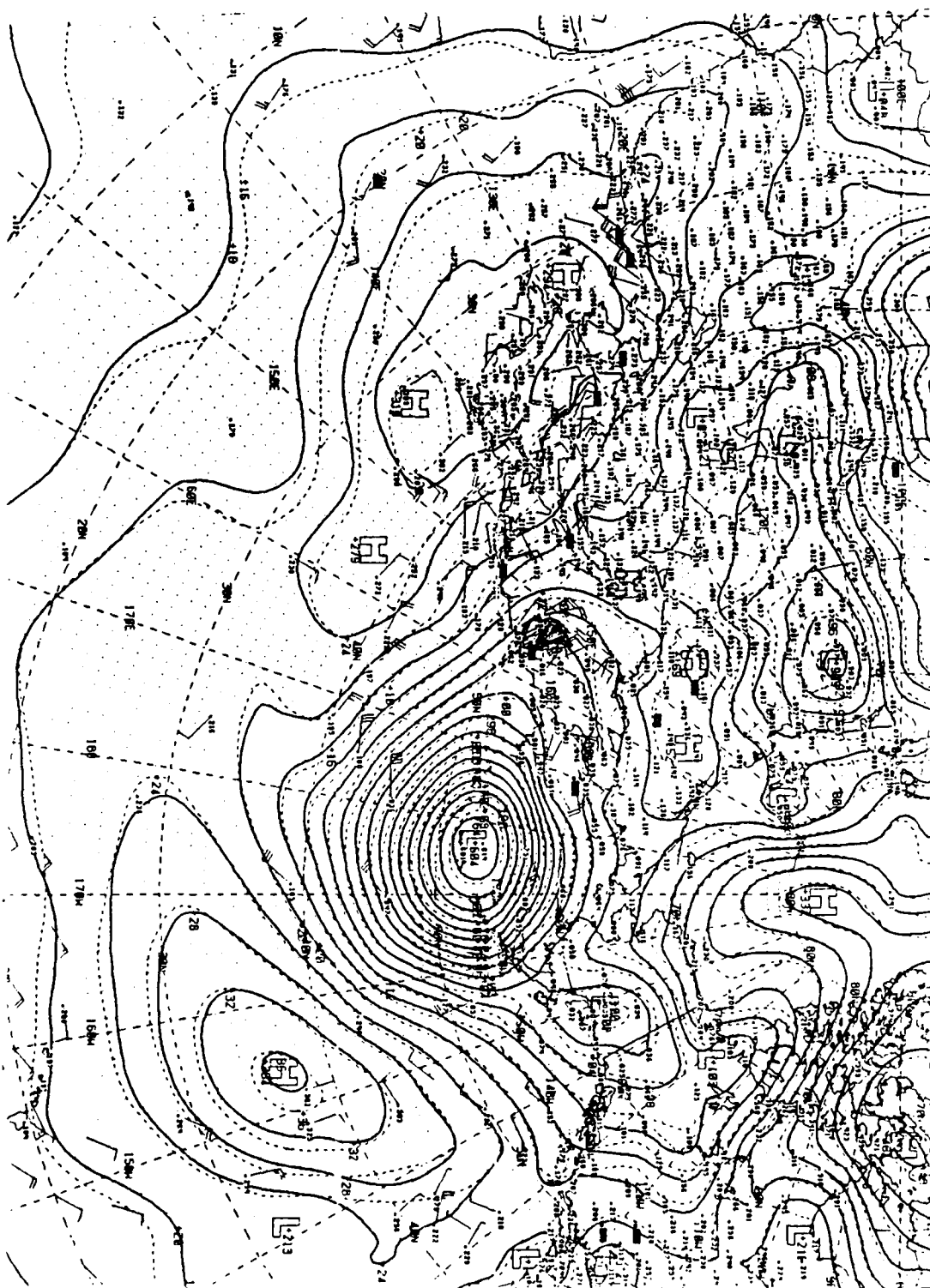


Figure 4.1: NOGAPS 1200 UTC 10 April 1988 Surface Analysis

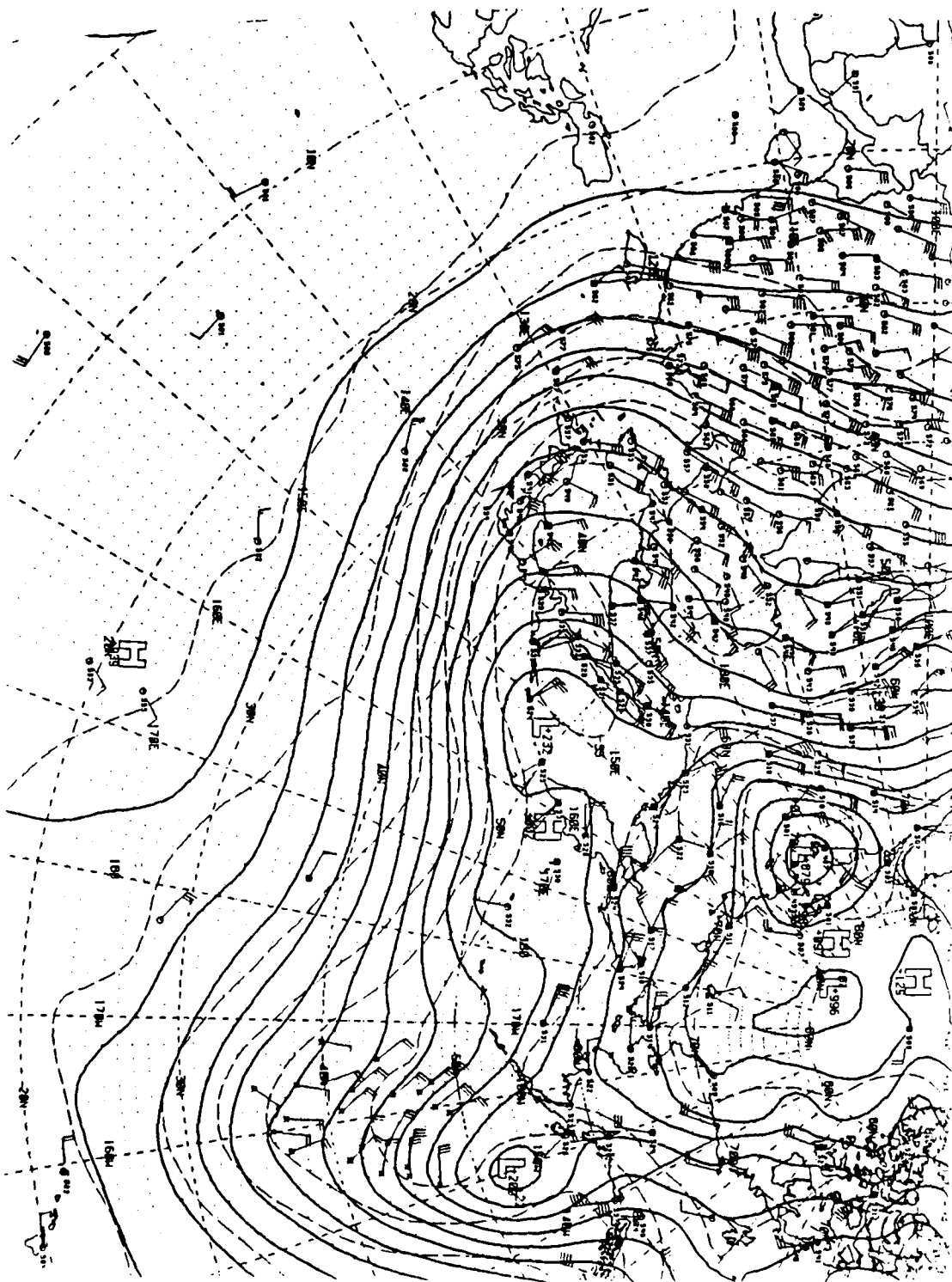


Figure 4.2: NOGAPS 1200 UTC 10 April 1988 500 mb Analysis

One of the important features affecting the aerosol concentrations in this region is the strong westerly flow pattern off the Asian continent, which provides a mechanism for the transport of continental and man-made aerosols. Another significant feature is the strong low pressure system centered around 50° N and 170° W. This storm system greatly inhibited the shipboard measurements in the 40° to 50° N region and limited the amount of data available for verification against satellite measurements. Fig. 4.3 shows the number of clear observations obtained by the satellite within a ± 3 day period of the ship's position. The choice of a 3-day band provides a complete data set for comparison with shipboard observations. If a shorter time period was utilized, data gaps would exist in the region of 38-44° N due to the strong cyclone. Choice of a longer period would result in the satellite data less accurately reflecting the in-situ data measured at the surface.

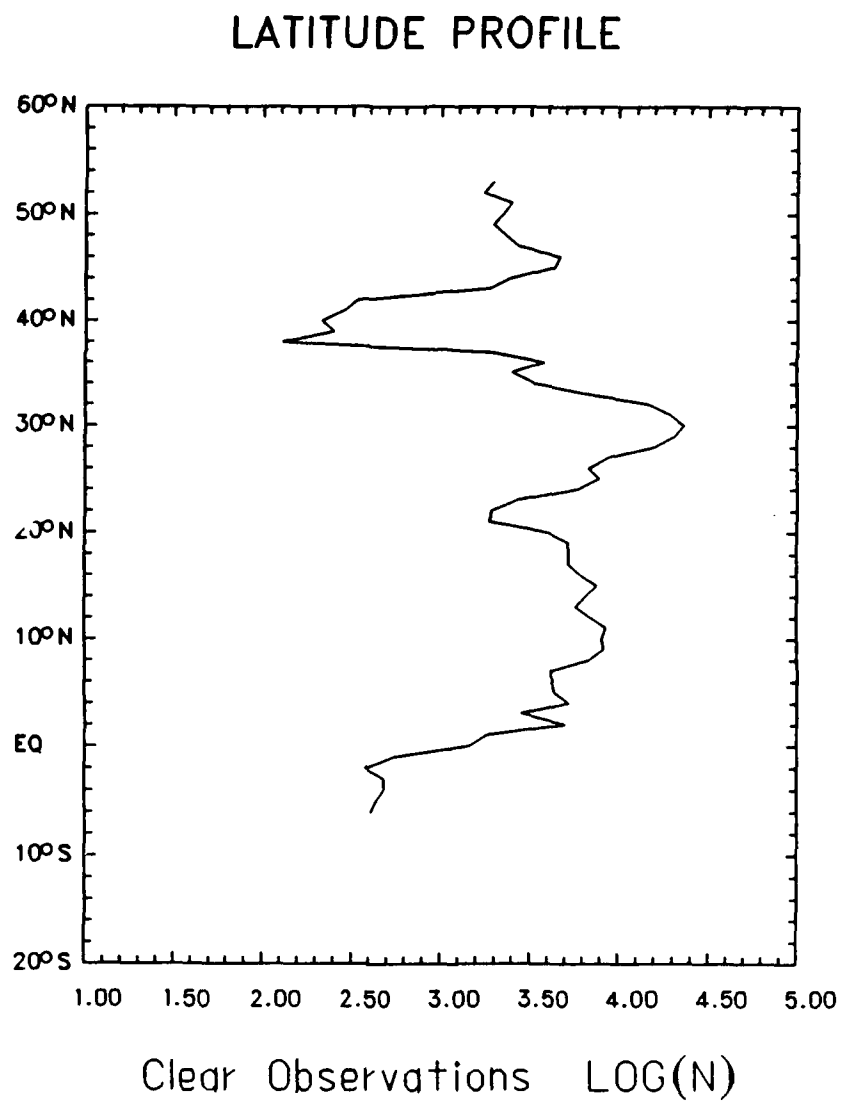


Figure 4.3: Number of Clear Observations - Values are within ± 3 days of Ship's Position

The last significant synoptic feature to identify is in the region south of 20° N where NE trade winds dominate during this period. In the region of the Hawaiian Islands, this is especially important as it provides the primary transport mechanism for the volcanic emissions from Kilauea (19° N, 157° W).

B. AEROSOL SOURCES

In conjunction with the synoptic situation, another key to the study of aerosol variations are the environmental influences. Two major influences are present in this region during the April 1988 period. These are desert dust storms and volcanic emissions.

"Kosa" is the phenomenon in which dust clouds originating from storms in the Gobi desert transport large quantities of dust through the atmosphere. Murayama (1987) showed that April is the highest frequency of these dust storms. During the period of this study, two significant "Kosa" occurred, which could, when coupled with the synoptic situation, affect aerosol measurements in the central North Pacific Region. Shaw (1980) has shown that with a nominal zonal translation of 1000 km/day, dust from storms in the Gobi desert could easily reach the central North Pacific. Therefore, these dust storms should have a major impact on aerosol particle concentration in the region studied.

Fig. 4.4 and 4.5 show the four-day transport of particles from these storms measured by the geostationary meteorological satellite (GMS). In Fig. 4.4, the dust storm originates on 10 April 1988 at 40° N, 140° E. In Fig. 4.5, a similar dust storm occurs originating on 16 April 1988 at 42° N, 105° E and results in atmospheric dust transport to a region centered at 38° N, 132° E.

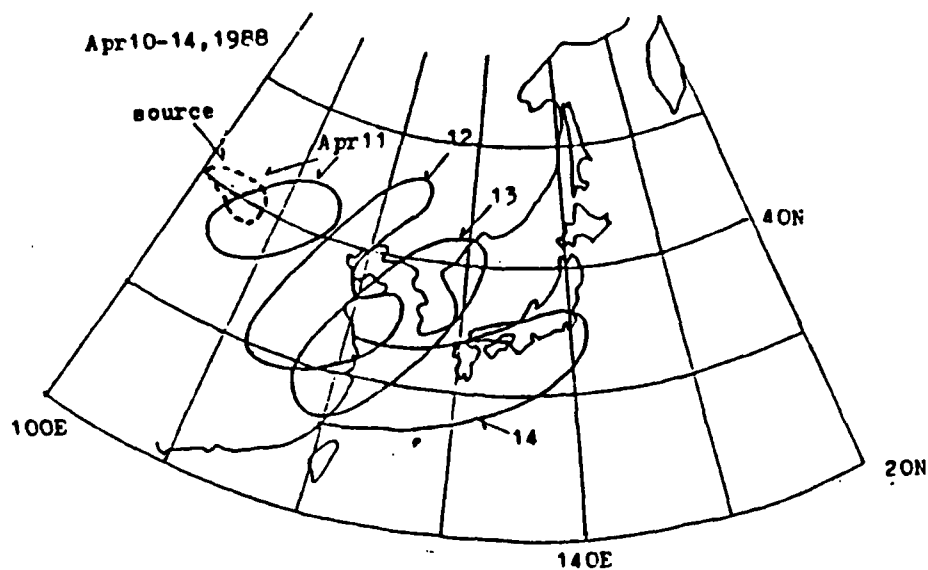


Figure 4.4: "Kosa" Transport Mechanism, 10-14 April 1988, from Murayama (1988)

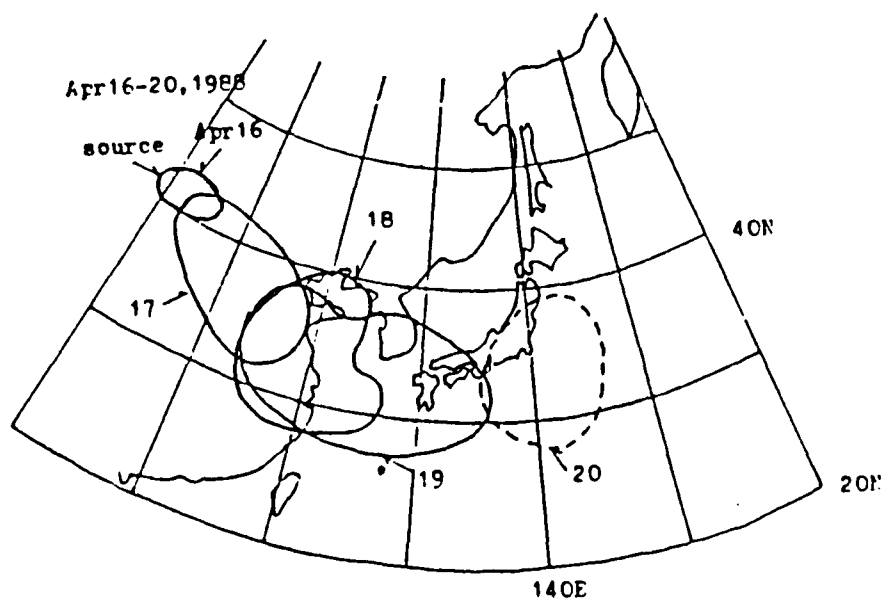


Figure 4.5: "Kosa" Transport Mechanism, 16-20 April 1988, from Murayama (1988)

The second major aerosol producing event is the eruption of the Kilauea volcano on the island of Hawaii (19° N, 157° W). Debris from this eruption was carried by the NE trade winds across the track of R/V OCEANOGRAPHER and should have a significant effect on the aerosol measurements and allow for verification of satellite retrieval techniques and aerosol transport mechanisms.

Fig. 4.6 is the aerosol optical depth composite for the region from latitude 50° N to 12° S and from longitude 140° W to 160° E for the period 7 April to 5 May 1988.

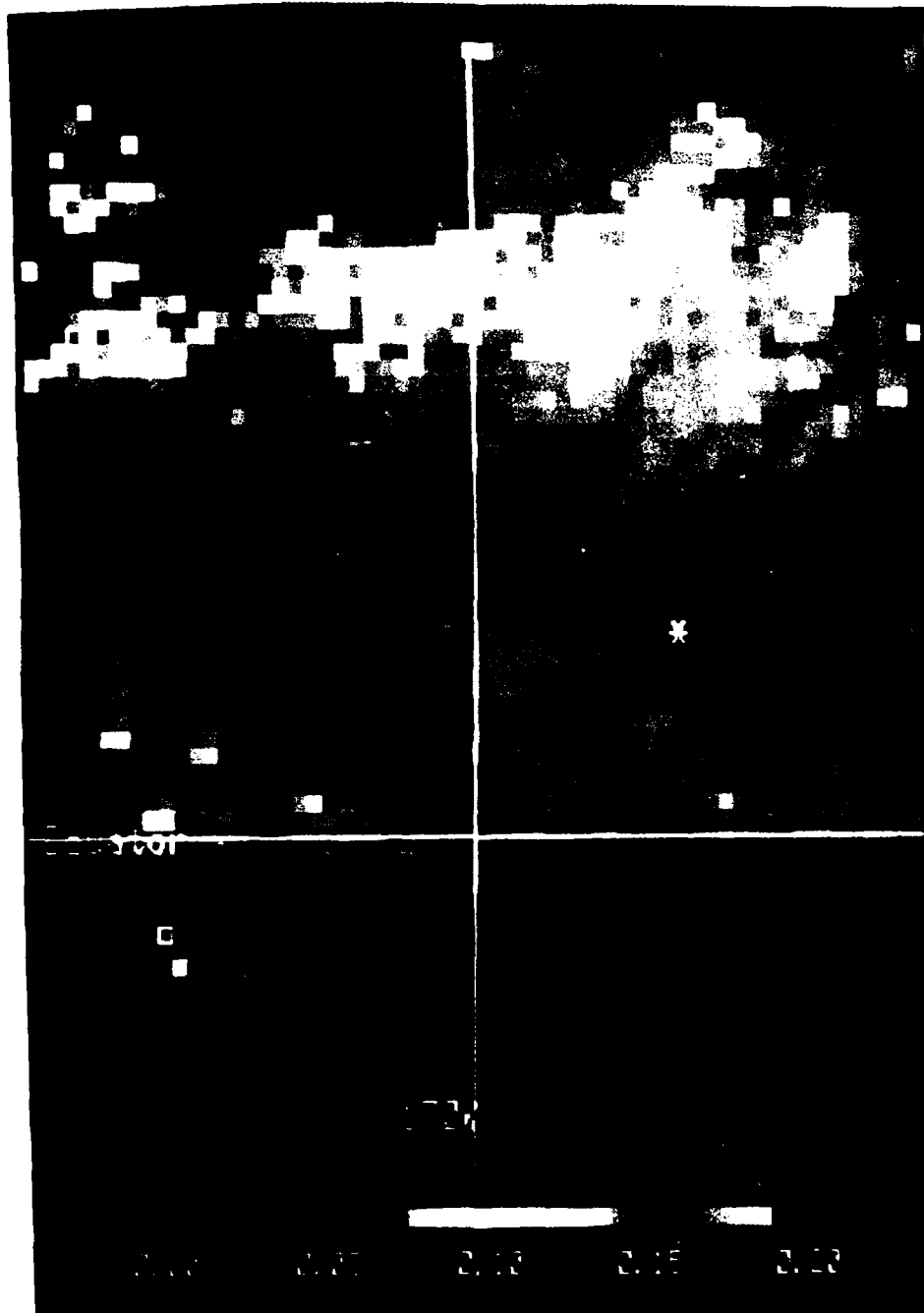


Figure 4.6: Optical Depth Composite. Data taken from NOAA-9 AVHRR during April 1988

In this figure, there are consistently high values for optical depth in the 0.1 to 0.2 range along the 35° to 45° N latitude band. This is indicative of the transport of continental sources by the predominant synoptic flow pattern in the western North Pacific. The second key feature is near the Hawaiian Islands depicted by an * in the figure. In the 18° to 20° N latitude band, the optical depth increases and spreads out as the volcano emissions are transported southwest by the synoptic flow pattern. This indicates that either the particles are increasing in size as they move away from the source or variations in the rate of emission may be occurring. Fig. 4.7 is the S_{12} composite for the same region and time period as the optical depth composite.

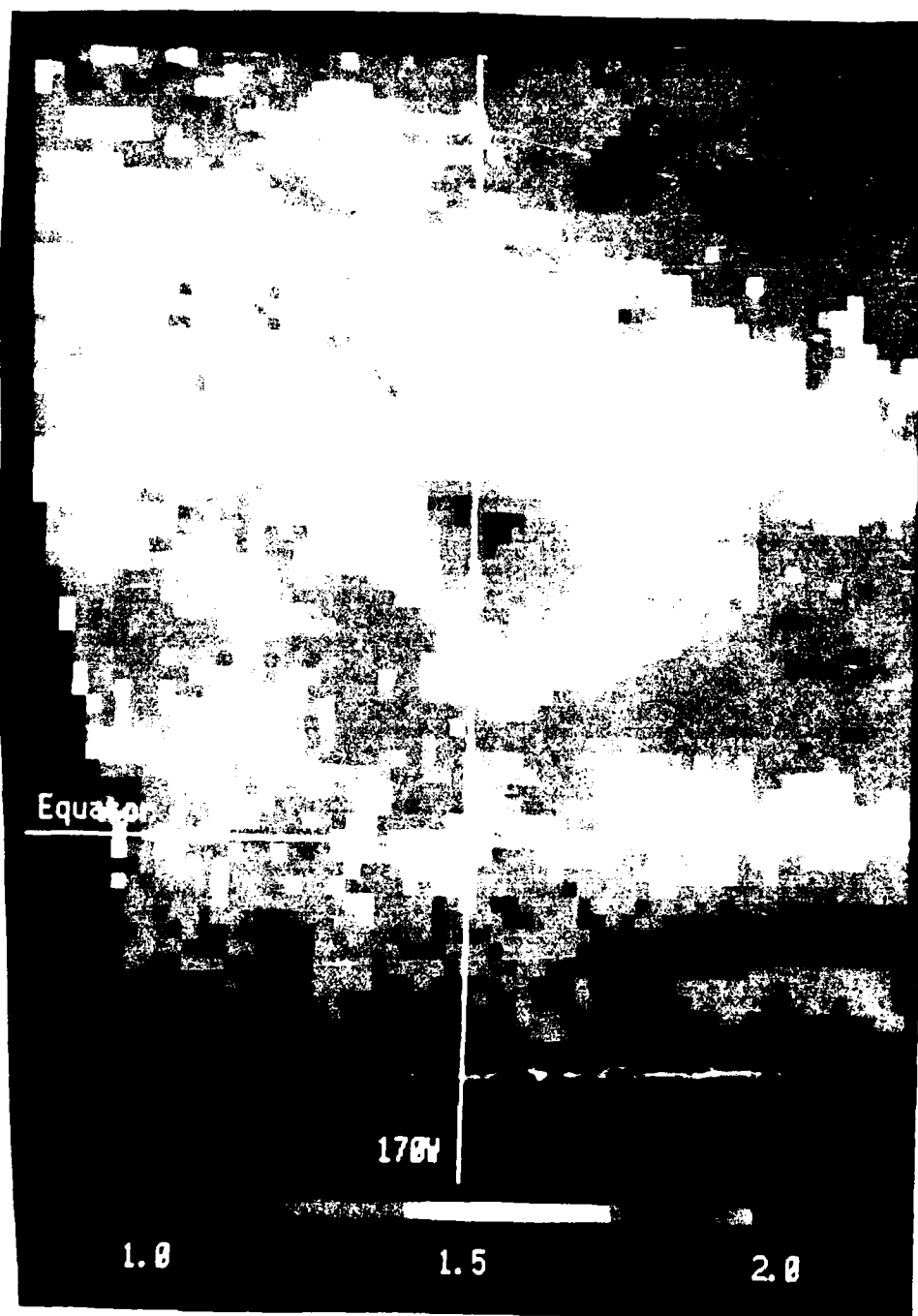


Figure 4.7: S_{12} Composite. Data compiled from NOAA-9 AVHRR during April 1988

In the 35-45° N band high S_{12} values are collocated with the high optical depth values. This is indicative of a very large number of aerosol particles in the atmosphere. The high S_{12} values in this same region mean that there are scattering agents present. The high S_{12} values in this same region show that the distribution of the aerosol particles are weighted towards smaller particles. Therefore, it is reasonable to conclude that large amounts of aerosols, continental in origin, are blowing off the land and out over water into this region. In the 18-20° N latitude band near the Hawaiian Islands, S_{12} values are decreasing as the volcanic emissions spread westward. This indicates that the ratio of small particles to large particles is decreasing. When combined with the results of the optical depth increase for the same area, it appears that the aerosol particles are increasing in size as they transport westward through the atmosphere.

C. INTERCOMPARISON OF OPTICAL DEPTH AND CONDENSATION NUCLEI

Optical depth measured from a satellite gives an understanding of the transmittance capabilities of the entire atmospheric layer, whereas shipboard measurements are confined to the surface boundary layer. Nevertheless, a strong indicator of the validity of satellite retrieval techniques should be obtained based upon a positive correlation between shipboard and satellite measurements. Previously, it was shown that changes in aerosol particle distribution detected by the satellite are a function of the optical depth. In-situ measurements of condensation nuclei are a function of the surface boundary layer distribution of aerosol particles. Therefore, if satellite retrieval methods are correct, a positive correlation should exist between optical depth and condensation nuclei measurements to the extent that the surface reflects the tropospheric changes.

Fig. 4.8 shows the optical depths obtained from the satellite measurements utilizing a ± 3 day variation from the ship's position. Optical depth maximums occur at 45° N to 35° N, 20° N, 10° N, and 2° N. Additionally, optical depth values are minimal in the region south of 2° N, with satellite data not available south of 6° S. Fig. 4.9 shows the condensation nuclei count for the same period measured on the R/V OCEANOGRAPHER. Similar peaks are observed as with the optical depth values. However, there is some variation in their location. There are several reasons for these variations in peak location. The primary reason is that satellite measurements are integrated over the entire atmosphere, whereas condensation nuclei are counted at the surface. Therefore, aerosol particles transported into the region from distant continental sources should cause a higher optical depth. The second reason is that the condensation nuclei count is the sum of all particles whose $n(r)$ peaks at a value of $.1 \mu\text{m}$. The δ_A is the sum of all particles weighted by scattering efficiency peaks at $.63 \mu\text{m}$, therefore, the δ_A is sensitive to a larger radius particle than CN measurements. Utilizing a Pearson correlation moment (Walpole and Meyers 1985), the correlation for the two data sets is 0.56 for 59 samples. This positive correlation is a strong indicator of the validity of satellite retrieval techniques. Further examination of Fig. 4.8 and 4.9 reveal that the largest values for optical depth and condensation nuclei occur in the 10 - 50° N band, while the smallest values with the least variation occur south of 10° N. By separating the data into a North data set, the correlation coefficient was a positive correlation of 0.6 for 42 samples. For the South data set, there was a negative correlation of 0.44 for 17 samples. This negative correlation is indicative of the small data set with little variation and the differences between sensitivity of CN counts and δ_A measurements.

The second largest feature for both optical depth and condensation nuclei is centered at 20° N. The major aerosol producing event in this region is the eruption

of the Kilauea volcano. Positive correlation between the two data sets verifies the satellite retrieval techniques. Contrary to the Northern region, the CN count is larger and the optical depth is smaller. Optical depth increases when the number or radius of the aerosol particles increase. The CN count increases when the number of aerosol particles increase. Therefore, it appears there are a greater number of small particles in the atmosphere. This may be a reflection of the settling of the low-level debris out of the atmosphere as it moves away from the volcano or it may be that the aerosol optical depth is made up of particles with larger radii at 170° W. Therefore, with a weaker source, more of the optical depth is a function of higher altitude particles.

The peak at 10° N is most likely due to advection of continental sources by the prevailing NE trade winds (Bates and Charlson 1989). The change in optical depth and CN are three times smaller than in the westerly source off the Asian continent in the 40° N region. This appears to relate to the different type of continental source as well as to the effects of cloud processes in the tropical region. The peak near the Equator at 2° N is most likely biogenic in origin and is due to the upwelling, as there are no continental sources contributing in this region (Bates and Charlson 1989).

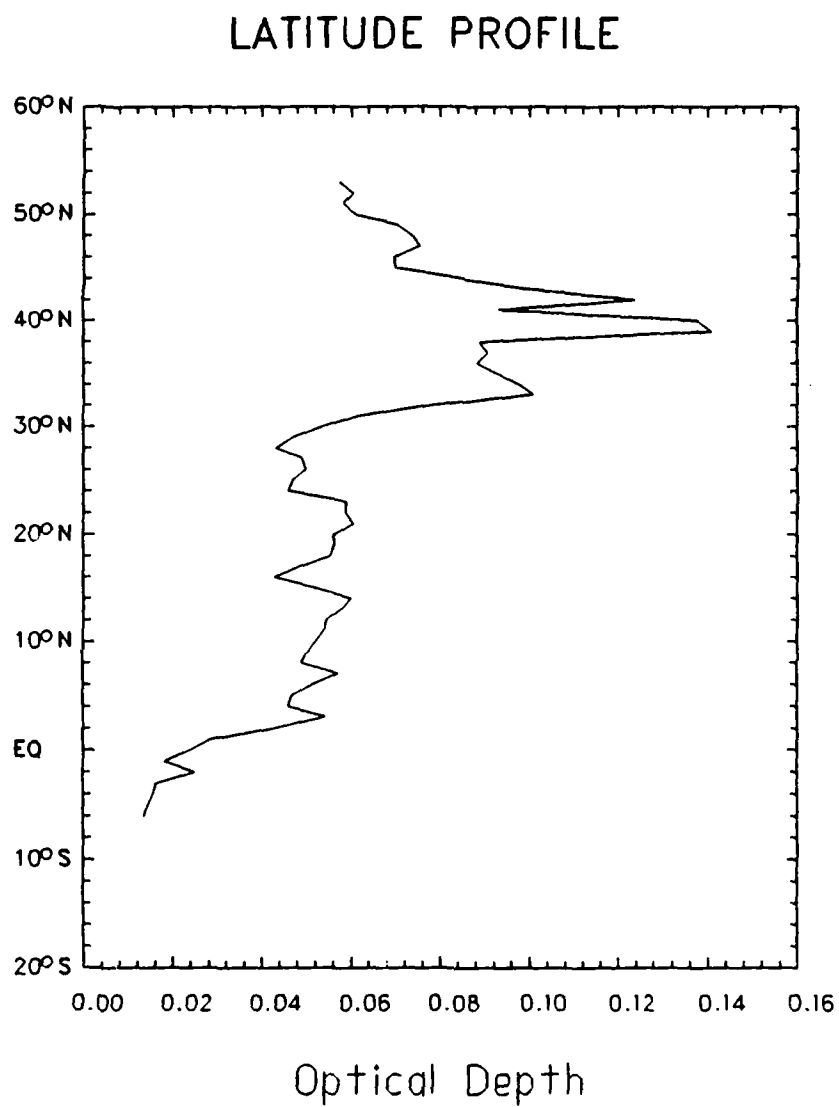


Figure 4.8: Optical Depth - Measured by NOAA-9 AVHRR within ± 3 days of Ship's Position

LATITUDE PROFILE

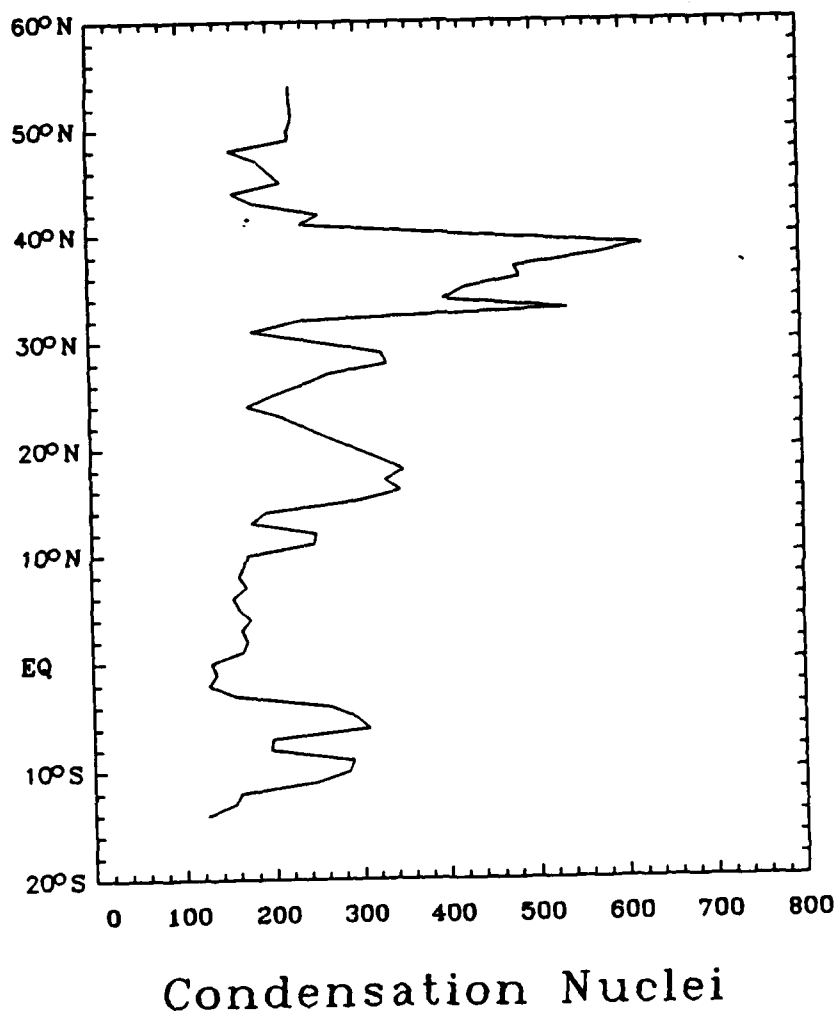


Figure 4.9: Condensation Nuclei - Measured by the R/V OCEANOGRAPHER

D. INTERCOMPARISON OF S_{12} RATIO AND NSS-SO_4^{2-}

Fig. 4.10 shows that the dominate features for the S_{12} are maximums at 35° N, 19° N, 10° N, 1° N, and 2° S. Recall from earlier discussions that these elevated values indicate a greater ratio of small particles to large particles in the atmospheric distribution. Charlson, et al., (1987) describe a mechanism in which high oceanic DMS productivity by phytoplankton relates to increased numbers of small aerosol particles in the atmosphere. Therefore, one could infer that increased DMS productivity in a region (and the resultant increase in NSS-SO_4^{2-}) should correlate with increased S_{12} values. However, there are several factors which influence such a direct correlation. First, it has been shown that the primary sources for aerosols in the atmosphere for the North Pacific region (10 - 45° N) of this study are anthropogenic, volcanic, or originate from atmospheric transport of Gobi desert dust storms. Therefore, biogenic activity in this region is either extremely limited or overshadowed by the continental sources. Second, the North Pacific Ocean region is noted for its reduced DMS productivity (Gross 1972). Third, during the cruise of the R/V OCEANOGRAPHER, it was noted that DMS production was at a winter low (Bates and Charlson 1989). Therefore, a direct correlation between DMS and S_{12} is not seen in the North Pacific.

In the equatorial region, the aerosol particles appear to be biogenic in origin. This is because the Inter-Tropical Convergence Zone (ITCZ) appears to be an effective removal mechanism for continental sources of aerosols (Clarke 1989). Andrea (1985) found that DMS concentrations are very high in upwelled tropical waters. Additionally, Clarke (1987) observed that DMS production in the equatorial region is 3-5 times greater than in the North Pacific. Therefore, it is reasonable to expect that the NSS-SO_4^{2-} aerosols are biogenic in origin.

Fig. 4.11 shows the NSS-SO_4^{2-} data obtained from shipboard measurements on the R/V OCEANOGRAPHER. In the equatorial region, as expected, there is a maximum in sulfate measurements from 4° N to 2° S . The presence of this sulfate aerosol over such an extensive region remote from continental sources is consistent with production by biogenic sources such as DMS. The satellite derived S_{12} has peak values at 1° N and 2° S and, in conjunction with the low optical depths for this area, from Fig. 4.8 provide strong support that these particles are biogenic in origin. It also coincides with Clarke (1987) in that there is an increase in atmospheric sulfur compounds in the equatorial region. Shipboard measurements of condensation nuclei also showed an increase in this region. This supports Charlson's hypothesis concerning increased oceanic DMS production.

The most prominent feature in Fig. 4.11 is the large peak in sulfate particles in the 20° N region. This maximum is a result of the volcanic emissions from the Kilauea volcano, and correlates with a similar maximum in S_{12} at 20° N .

Shipboard sulfate measurements in the region of 40° N were limited due to the high winds and rough seas encountered. With the continental aerosol input from the westerly flow, it would be reasonable to expect higher NSS-SO_4^{2-} values. However, the aerosol particles in this region may not be sulfur based, which is indicative of atmospheric dust transport vice combustion sources from the Asian continent. Also, the S_{12} at 40° N is smaller, therefore, indicating that there are more large particles. Additionally, the maximum in S_{12} located at 35° N may indicate that this region is anthropogenic in origin. The $38\text{-}44^\circ \text{ N}$ region maximums for both optical depth and condensation nuclei confirm the presence of a large number of aerosol particles in this region. The source of these particles is the westerly transport of continental and man-made aerosols due to the westerly synoptic flow pattern previously discussed. Interestingly, the peaks in optical depth at 42° N and 39° N probably represent

separate sources. The 42° N peak with a smaller optical depth than at 39° N has a larger APSI as shown in Fig. 4.10. The larger APSI with smaller optical depth indicates a greater number of smaller particles which would probably be of man-made origin. Conversely, the peak at 39° N has a larger optical depth with a smaller S_{12} , therefore, the aerosols are larger and of a different source, most likely the Gobi desert "Kosa".

The last feature to discuss is the corresponding peaks at 10° N for sulfate measurements and S_{12} . The most likely source for these peaks is the NE tradewinds transporting continental sources of aerosols. The correlation of the above data points is another strong verification of the satellite retrieval methods.

LATITUDE PROFILE

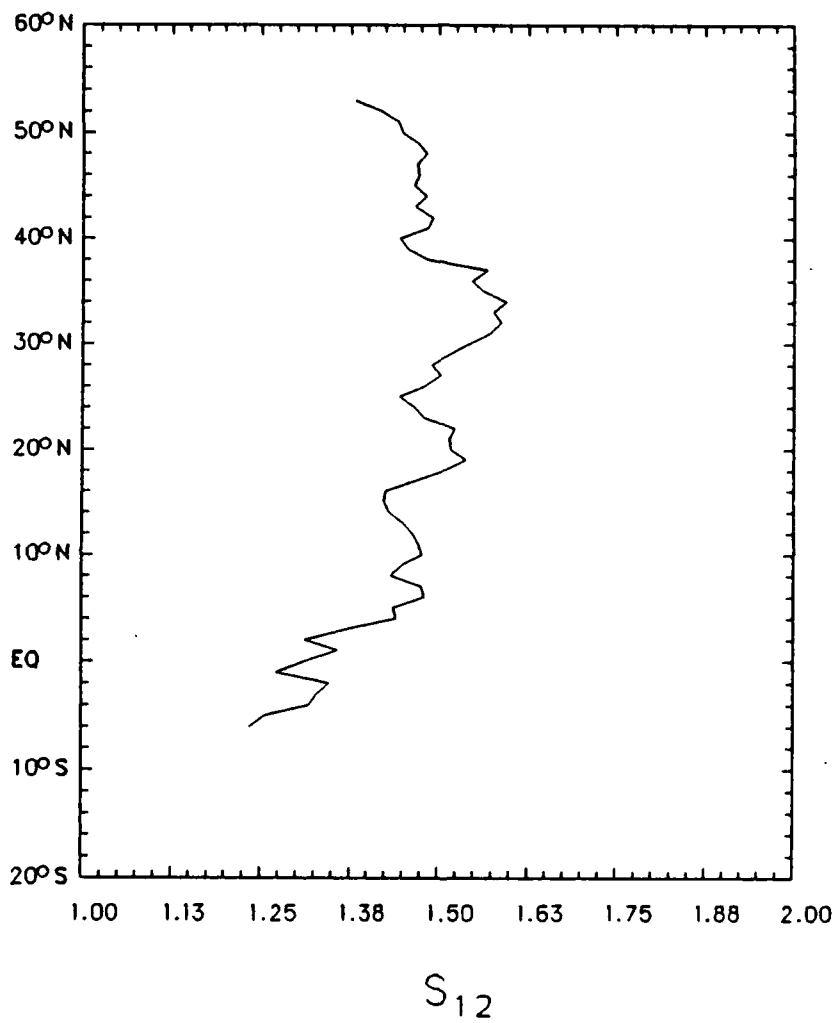


Figure 4.10: S_{12} Ratio - Measured by NOAA-9 AVHRR within ± 3 days of Ship's Position

LATITUDE PROFILE

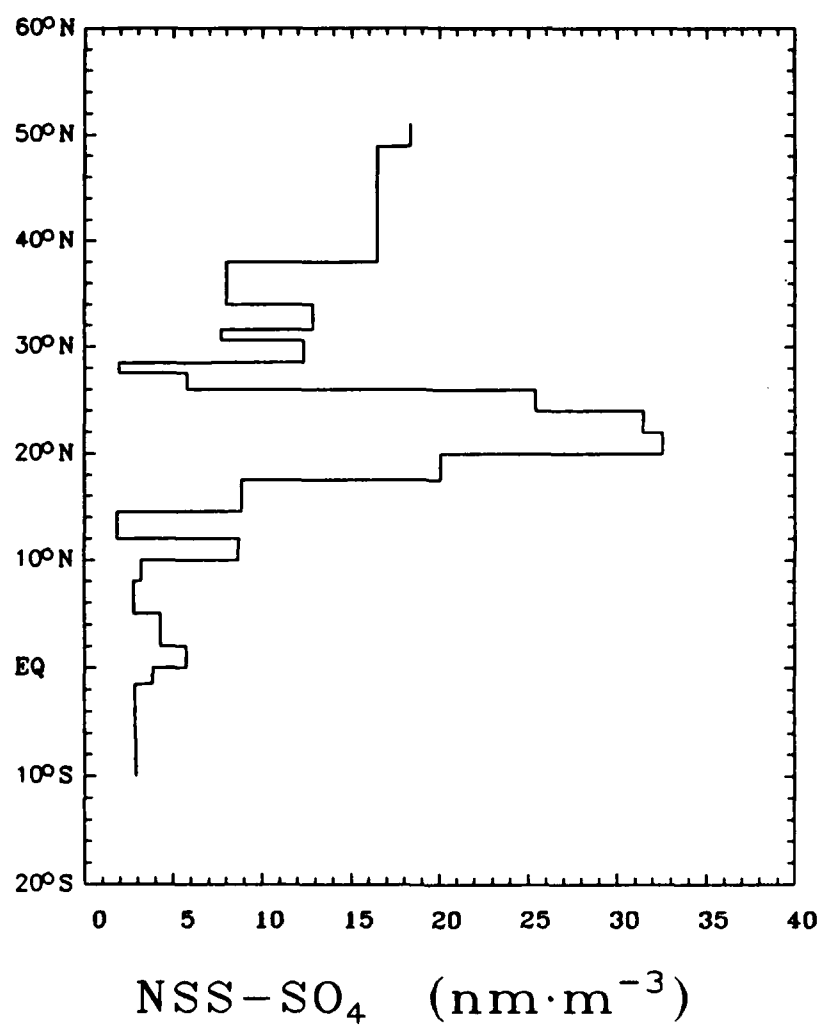


Figure 4.11: NSS-SO₄²⁻ Data - Measurements made by R/V OCEANOGRAPHER during April 1988

E. CHANNEL 1 AND CHANNEL 3 LOW CLOUD REFLECTANCE

Fig. 4.12 is the channel 1 ($0.63 \mu\text{m}$) low cloud reflectance data for the entire period. There is very little variation in the channel 1 reflectance values. Recall that the magnitude of the reflectance in this portion of the electromagnetic spectrum is heavily dependent upon cloud thickness and liquid water content (LWC) of the cloud, as well as the droplet size distribution. Therefore, these three variables must be offsetting each other, and little change in the reflectance is noted over the entire region. It is extremely difficult to obtain a correlation between reflectance and cloud droplet size in this channel. Fig. 4.13 and 4.14 are composite optical depths and S_{12} measured by the satellite for the entire period. Higher optical depths and S_{12} values are noted in the $10\text{-}40^\circ \text{N}$ region. This would indicate that there are a greater number of aerosol particles with a smaller mean radius in the northern regions. Also, shipboard measurements of condensation nuclei increased in the northern region of this study. Channel 1 low cloud reflectance values do not show any effect of this variability.

For channel 3 ($3.7 \mu\text{m}$) reflectance, recall that the dependence on LWC and cloud thickness is not nearly as great as the dependence on droplet radius. Fig. 4.15 is the low cloud reflectance of the entire region of this study. It is a significant result that low cloud reflectance is increasing from $10\text{-}40^\circ \text{N}$ with a maximum reflectance value at 42°N . This is a strong indicator that changes in cloud reflectance based on droplet size distribution is more observable using the channel 3 information and strongly supports the satellite retrieval techniques developed by Mincart (1988).

When CN (Fig. 4.9) is compared to the channel 3 low cloud reflectance, there is a direct correlation in the region of maximum values. Therefore, as the number of CN increase, the number of CCN increase, and result in higher channel 3 low cloud

reflectance. This is clearly demonstrated at 20° N, where the increase in CN due to volcanic activity results in channel 3 reflectivity increases.

LATITUDE PROFILE

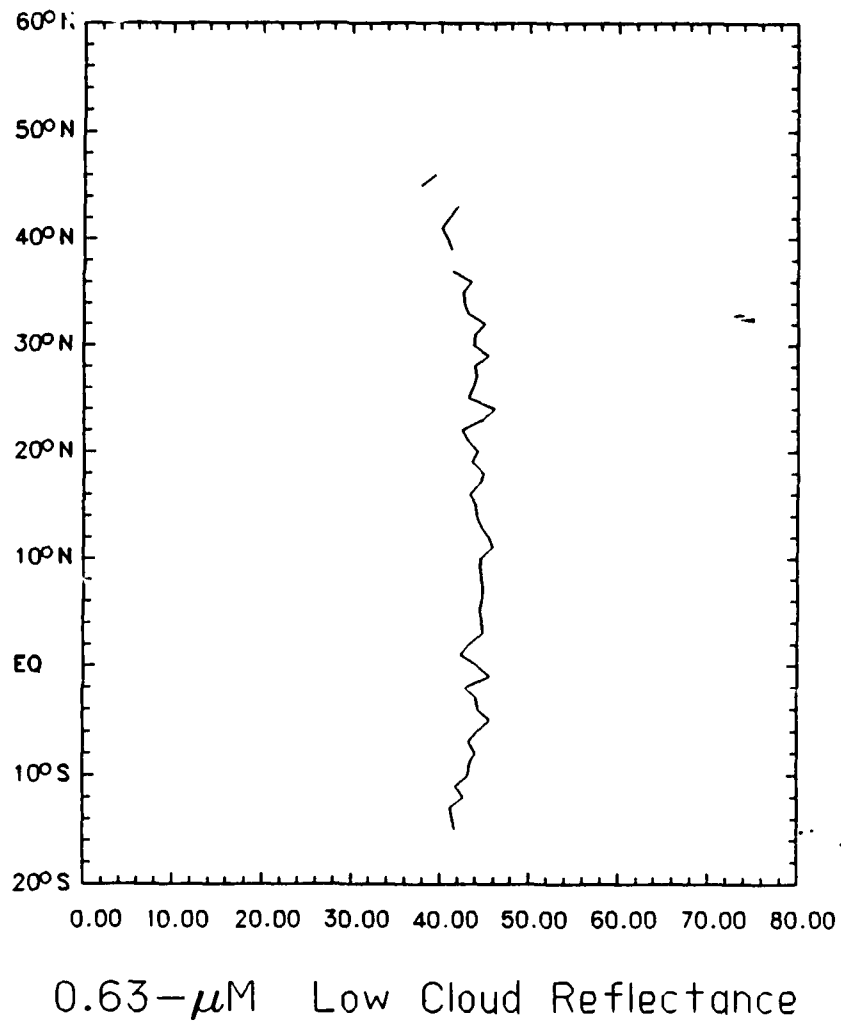


Figure 4.12: Channel 1 Low Cloud Reflectance - Measured by NOAA-9 AVHRR

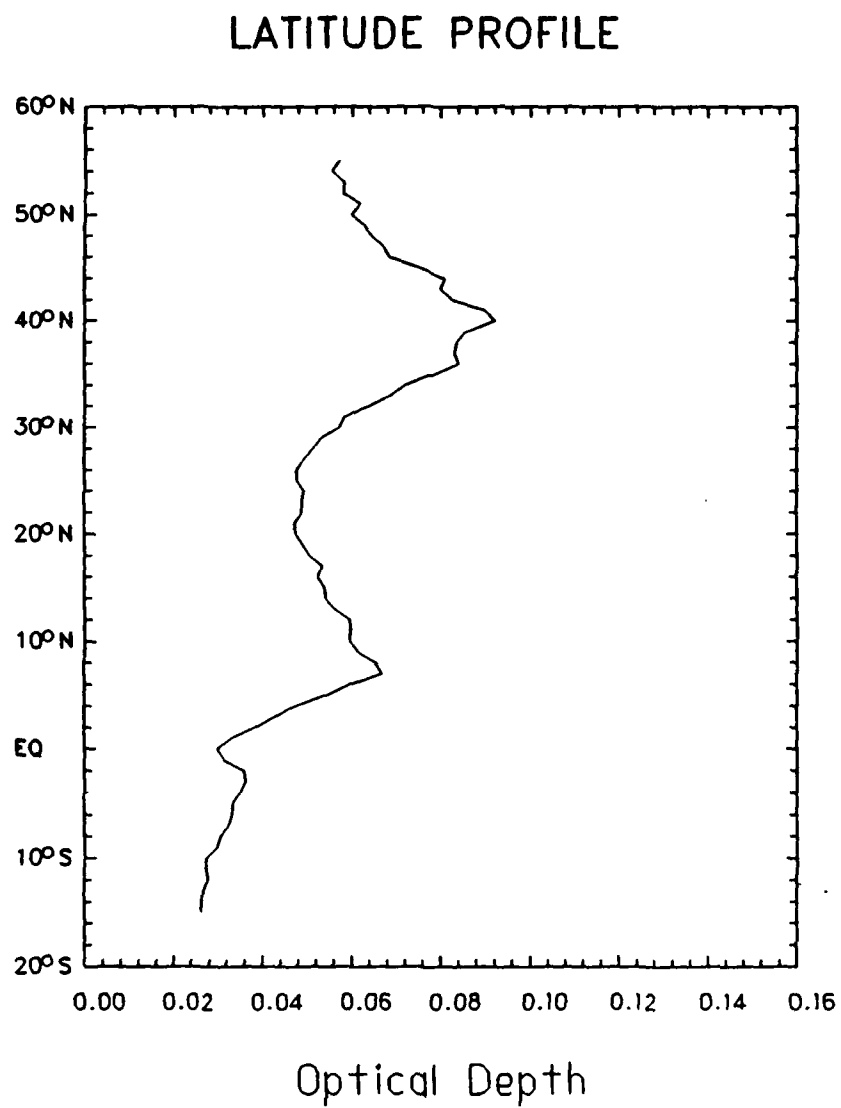


Figure 4.13: Composite Optical Depth - Measured by NOAA-9 AVHRR

LATITUDE PROFILE

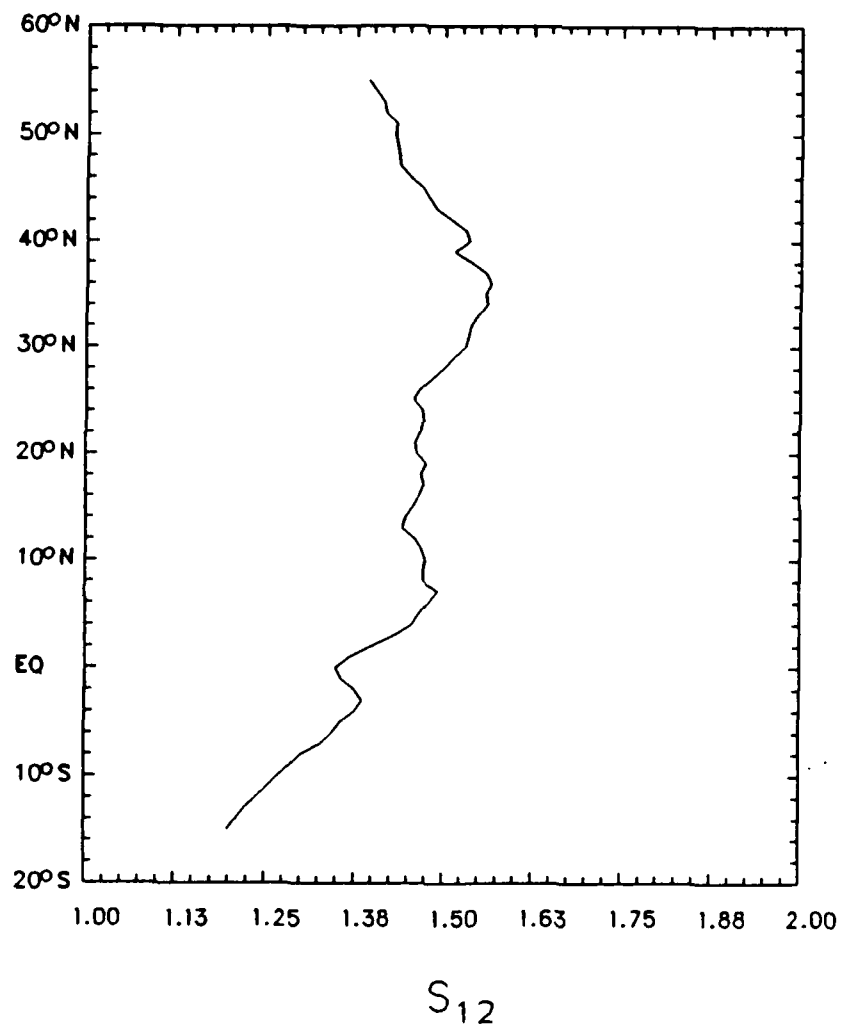
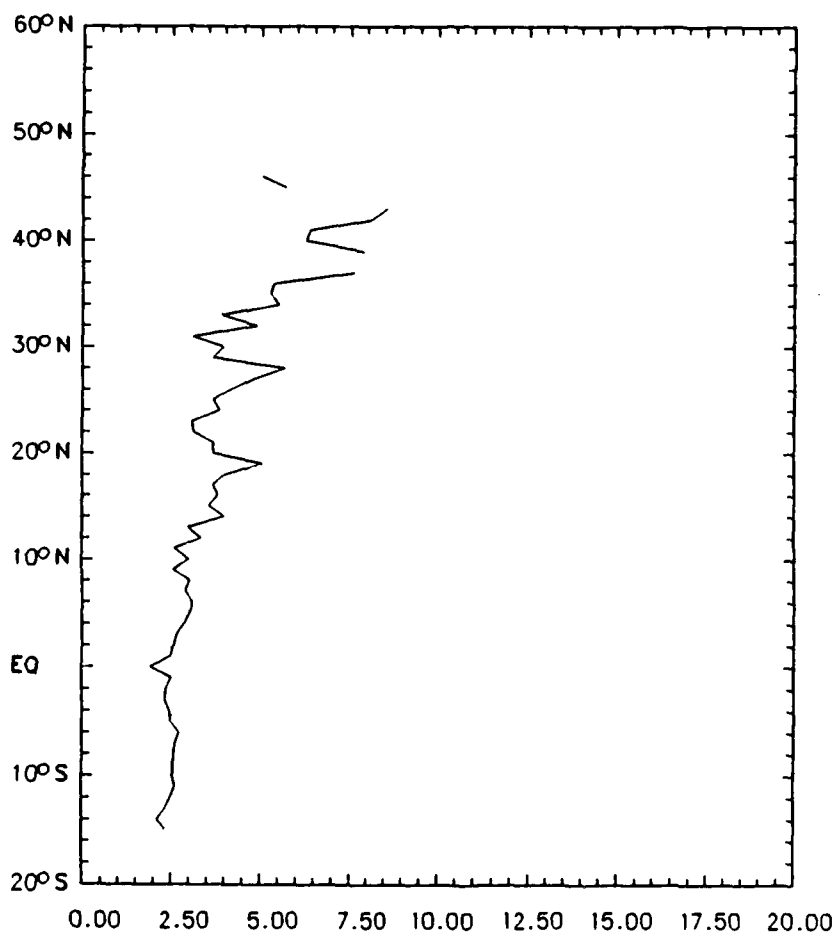


Figure 4.14: Composite S_{12} - Measured by NOAA-9 AVHRR

LATITUDE PROFILE



3.7- μ M Low Cloud Reflectance

Figure 4.15: Channel 3 Low Cloud Reflectance - Measured by NOAA-9 AVHRR

V. CONCLUSIONS AND RECOMMENDATIONS

This study utilized data from the RITS-88 cruise and NOAA-9 AVHRR to verify satellite retrieval techniques, expand shipboard observations to a regional scale, and verify the relationship between aerosol characteristics and cloud reflectance properties. From these data, the aerosol characteristics were inferred and a better understanding of the radiative transfer properties of the atmosphere was obtained.

Optical depth values show a positive correlation with the shipboard condensation nuclei counts. This provides strong justification for utilizing satellite derived optical depth measurements when estimating the radiative transfer characteristics of a region. When combined with the S_{12} values, these two techniques are very useful in determining the type and quantity of aerosols in the atmosphere. This would provide valuable information to global climate studies, as well as to the effects of aerosols on electro-optical systems.

The relationship between solar reflectance and cloud droplet size distribution was illustrated. High channel 3 reflectivities are associated with high concentrations of aerosols, high concentrations of cloud droplets, and a shift toward smaller mean cloud droplet radius. This could provide a valuable tool for tracking the effects of major events, such as forest fires, industrial accidents, or volcanic emissions effect on the environment.

The expansion of shipboard data to a regional scale via satellite measurements resulted in the identification of several strong aerosol sources in the North Pacific. In conjunction with this, it provided more evidence of the ability of the atmosphere to transport aerosol particles great distances. The volcanic plume from Kilauea volcano

was identified as a significant aerosol producing source for this region. The two major events of desert duststorms and volcanic emissions highlighted how a spatial view of the relative aerosol size distribution was possible from the S_{12} and optical depth data. This made it relatively easy to distinguish between anthropogenic and naturally occurring aerosols. This would not have been possible utilizing only in-situ shipboard data and it highlights the valuable contribution of satellite retrieval methodology.

Savoie and Prospero (1989) proposed that NSS-SO_4^{2-} concentrations over the Pacific appear to be primarily controlled by biogenic sources in the ocean. Contrary to their conclusions, during the time period of this study, continental sources of aerosols had a greater impact in the North Pacific region. Continental influences would hinder any efforts to examine the relationship of DMS production to increasing the number of CCN in the atmosphere. Shema (1988) proposed that the equatorial region is a better place to study the relationships between DMS, aerosols, and clouds. Clarke (1989) proposed that the ITCZ appears to filter out continental sources of aerosols in the equatorial region. As a result, the aerosol particle population is mainly biogenic in origin, which are precursors to DMS production. Therefore, the study of Charlson's biological feedback mechanism would be greatly enhanced in this region.

The simple satellite retrieval techniques utilized in this study show that the effect of changing cloud reflectance due to spatial variations in aerosol concentration and composition can be incorporated into global climate studies using archived AVHRR data.

Recommendations for future studies of this nature should compare in-situ measurements over the entire troposphere versus satellite data and incorporate CCN

measurements. This will give a better representation of the validity of satellite retrieval techniques.

LIST OF REFERENCES

- Andrea, M. O., 1985: Dimethylsulfide in the water column and sediment pore waters of the Peru upwelling area. *Limnol. Oceanogr.*, **30**(6), 1208-1218.
- Bates, T. S. and Charlson, R. J., January 29, 1989: The role of the sulfur cycle in cloud microphysics, cloud albedo, and climate. Extended abstract for the American Meteorological Society 69th Annual Meeting.
- Bloembergen, N., Patel, C. K., and Pake, G. (Chairpersons), 1987: Science and Technology of Directed Energy Weapons. Report of the American Physical Society Study Group, *Reviews of Modern Physics*, **59**, S1-S202.
- Charlson, R. J., Lovelock, J. E., Andrea, M. O., and Warren, S. G., 1987: Oceanic phytoplankton, atmospheric sulfur, cloud albedo and climate. *Nature*, **325**, 655-661.
- Clarke, A. D., 1987: The Pacific marine aerosol: evidence for natural acid sulfates. *J. Geophys. Res.*, **92**(D4), 4179-4190.
- Clarke, A. D., November 1989: Interhemispheric gradients in aerosol properties over the Pacific. Personal communication.
- Coakley, J. A., Jr., and Davies, R., 1986: The effects of cloud sides on reflected solar radiation as deduced from satellite observations. *J. Atmos. Sci.*, **43**, 1025-1035.
- Coakley, J. A., Jr., Cess, R. D., and Yurevich, F. B., 1983: The effect of tropospheric aerosols on the earth's radiation budget: A parameterization for climate models. *J. Atmos. Sci.*, **40**, 116-138.
- Cordray, D. M., Fitzgerald, J. W., Gathman, S. G., Hayes, J. N., Kenney, J. E., Mueller, G. P., and Ruskin, R. E., 1977: Meteorological Sensitivity Study on High Energy Laser Propagation. Naval Research Laboratory Report 8097, Washington, D.C. 81pp.
- Durkee, P. A., 1984: *The relationship between marine aerosol particles and satellite-detected radiance*. Ph.D. dissertation, Colorado State University, Fort Collins, CO. US ISSN 0067-0340, 124pp.
- Durkee, P. A., Jensen, D. R., Hindman, E. E., and Vondor Harr, T. H., 1986: The relationship between marine aerosol particles and satellite-detected radiance. *J. Geophys. Res.*, **91**(D3), 4063-4072.
- Frost, E. M., 1988: *Global scale estimates of aerosol particle characteristics*. M.S. Thesis, Naval Postgraduate School, Monterey, CA., 54pp.
- Gross, M. G., 1972: *Oceanography - a view of the earth*. Prentice-Hall, New Jersey, 497pp.

Kidwell, K. B., 1986: *NOAA Polar Orbiter Users Guide*, National Environmental Satellite Data and Information Service, Washington D.C., 120pp.

Milton, A. F., Harvey, G. L., and Schmidt, A. W., 1977: Comparison of the 3-5 micrometer and 8-12 micrometer Regions for Advanced Thermal Imaging Systems: LOWTRAN Revisited. Naval Research Laboratory Report 8172, Washington, D.C., 35pp.

Mineart, G. M., 1988: *Multispectral satellite analysis of marine stratocumulus cloud microphysics*. M.S. Thesis, Naval Postgraduate School, Monterey, CA, 138pp.

Murayama, N., 1987: *Kosa and dust/sand storm produced aerosols, Integrated Technique of Instrumentation and Control of Airborne Particulates for Air Cleaning*. R & D Planning, Tokyo, Japan, 288-332.

Murayama, N., 1988: *Dust clouds "Kosa" from the east Asian dust storms in 1982-1988 as observed by the GMS satellite*. Meteorological Satellite Center Technical Note No. 17, 10pp.

Pfiel, F. R., 1986: *Developing a physical basis for an aerosol climatology of the Pacific Ocean*. M.S. Thesis, Naval Postgraduate School, Monterey, CA, 75pp.

Pruppacher, H. R. and Klett, J. D., 1978: *Microphysics of clouds and precipitation*. Reidel, Dordrecht, 398pp.

Savoie, D. L. and Prospero, J. M., 1989: Comparison of oceanic and continental sources of non-sea-salt sulphate over the Pacific Ocean. *Nature*, **339**, 685-687.

Shaw, G. E., 1980: Transport of Asian desert aerosol to the Hawaiian Islands. *J. Appl. Meteor.*, **20**, 1254-1259.

Shema, R. A., 1988: *Correlation between satellite-derived aerosol characteristics and oceanic dimethylsulfide (DMS)*. M. S. Thesis, Naval Postgraduate School, Monterey, CA, 49pp.

Twomey, S., 1977: The influence of pollution on the shortwave albedo of clouds. *J. Atmos. Sci.*, **34**, 1148-1152.

Twomey, S., Piepgrass, M., and Wolfe, T. L., 1984: An assessment of the impact of pollution on global cloud albedo. *Tellus*, **36B**, 356-366.

Walpole, R. E. and Meyers, R. H., 1985: *Probability and Statistics for Engineers and Scientists*. MacMillan, New York, 639pp.

INITIAL DISTRIBUTION LIST

	No. of Copies
1. Defense Technical Information Center Cameron Station Alexandria, Virginia 22304-6145	2
2. Library, Code 0142 Naval Postgraduate School Monterey, California 93943-5002	2
3. Chairman, Code 63Rd Department of Meteorology Naval Postgraduate School Monterey, California 93943-5000	1
4. Chairman, Code 68Co Department of Oceanography Naval Postgraduate School Monterey, California 93943-5000	1
5. Professor Robert L. Haney, Code 63Hy Department of Meteorology Naval Postgraduate School Monterey, California 93943-5000	1
6. Professor Philip A. Durkee, Code 63De Department of Meteorology Naval Postgraduate School Monterey, California 93943-5000	2
7. Director, Naval Oceanography Division Naval Observatory 34th and Massachusetts Avenue NW Washington, D.C. 20390	1

- | | | |
|-----|---|---|
| 8. | Commander, Naval Oceanography Command
Stennis Space Center, Mississippi 39549-5000 | 1 |
| 9. | Commanding Officer
Naval Oceanographic Office
Stennis Space Center, Mississippi 39522-5001 | 1 |
| 10. | Commanding Officer
Fleet Numerical Oceanography Center
Monterey, California 93943-5010 | 1 |
| 11. | Commanding Officer
Naval Ocean Research and Development Activity
Stennis Space Center, Mississippi 39522-5001 | 1 |
| 12. | Commanding Officer
Naval Oceanographic and Atmospheric Research Laboratory
Monterey, California 93943-5011 | 1 |
| 13. | Chairman, Oceanography Department
U.S. Naval Academy
Annapolis, Maryland 21402 | 1 |
| 14. | Chief of Naval Research
800 North Quincy Street
Arlington, Virginia 22217 | 1 |
| 15. | Office of Naval Research, Code 420
Naval Ocean Research and Development Activity
800 North Quincy Street
Arlington, Virginia 22217 | 1 |
| 16. | Scientific Liaison Office
Office of Naval Research
Scripps Institution of Oceanography
La Jolla, California 92037 | 1 |

- | | | |
|-----|-------------------------------------|---|
| 17. | Library | 1 |
| | Scripps Institution of Oceanography | |
| | P.O. Box 2367 | |
| | La Jolla, California 92037 | |
| 18. | Library | 1 |
| | Department of Oceanography | |
| | University of Washington | |
| | Seattle, Washington 98105 | |
| 19. | LCDR Tod D. Benedict, USN | 2 |
| | Naval Western Oceanography Center | |
| | P.O. Box 113 | |
| | Pearl Harbor, Hawaii 96860-5050 | |